Basement-cover decoupling during the inversion of a hyperextended basin: Insights from the Eastern Pyrenees

Maxime Ducoux, Laurent Jolivet, Florence Cagnard, Thierry Baudin

Basement-cover decoupling during the inversion of a hyperextended basin: insights from the Eastern Pyrenees

M. Ducoux[1,2], L. Jolivet[3], F. Cagnard[4] & T. Baudin[4]

[1] ISTO, UMR7327, Université d'Orléans, CNRS, BRGM, F-45071 Orléans, France,

[2] Now at : M&U Sasu, 38120 SAINT-EGREVE, France

[3] Sorbonne Université, CNRS-INSU, Institut des Sciences de la Terre Paris, ISTeP UMR 7193, F-75005 Paris, France

[4] BRGM, F-45060 Orléans, France,

Abstract

Deformation processes related to early stages of collisional belts, especially the inversion of rifted systems remain poorly constrained, partly because evidence of these processes is usually obliterated during the subsequent collision. The Pyrenean belt resulting from the inversion of a Cretaceous hyperextended rifted margin associated with a H*T*/L*P* metamorphism in the Internal Metamorphic Zone (IMZ), is a good example for studying the early stage of orogenic deformation. This study is focused on the Eastern Pyrenees where the relation between inverted Mesozoic rifted basins and their basement are well-preserved. By using maximum temperatures (T_{max}) estimated by the Raman Spectroscopy of Carbonaceous Materials geothermometer and structural data, we describe the spatial distribution of the various tectono-metamorphic units. T_{max} recorded in the sedimentary cover exposed to the north and to the south of a Paleozoic basement block (Agly massif), exceed 550°C, while the Paleozoic metasediments and their autochthonous Mesozoic cover show T_{max} <350°C. The metamorphic sedimentary cover is affected by ductile deformation, while the basement is only affected by brittle deformation. Post-metamorphism breccias are observed between the basement and the metamorphic

This article has been accepted for publication and undergone full peer review but has not been through the copyediting, typesetting, pagination and proofreading process, which may lead to differences between this version and the Version of Record. Please cite this article as doi: 10.1029/2020TC006512.

sedimentary cover, which are interpreted as a decollement level in the Upper Triassic evaporites. Unlike previous models suggesting that the basement block separated two metamorphic basins (Boucheville and Bas Agly) during rifting, we propose a large displacement of a single metamorphic basin by a large thrust above the basement block. This novel interpretation emphasizes the general allochthonous position of the former hyperextended rift basin (IMZ) thrusted along a decoupling layer.

1. Introduction

It is commonly accepted that the major part of collisional orogens often results from the inversion and contraction of former continental rifted margins. However, the early stages of orogenic processes, corresponding to the inversion of the rifted system, usually affected by hyperextension, remains poorly constrained. The lack of knowledge on the early orogenic processes stems from the obliteration of the hyperextended part of former rift systems, during collision, by a strong metamorphic and tectonic overprint or because this domain is now buried in the crustal root of belts. Therefore, the inherited rift-related geometries and thermal-mechanical structure of the pre-orogenic crust and lithosphere play important roles in the structural style of collisional orogens (e.g. Lemoine et al., 1986; Watts *et al*., 1995; Mouthereau *et al*., 2013; Jammes & Huismans, 2012; Manatschal *et al*., 2015). Reconstructing the evolution of collisional belts and especially quantifying the finite shortening requires a precise understanding of their overall structure and kinematics, including the pre-orogenic position of the thrust packages. Recent studies have shown that the occurrence of salt tectonics during the pre-orogenic period can lead to significant overestimation of finite orogenic shortening (e.g. Jourdon et al., 2020; Izquierdo-Llavall et al., 2020; Labaume & Teixell, 2020). The timing of deposition of weak layers (salt-bearing rocks or shales), pre-, syn- or post-rift, is thus one of the main factors that controls the overall architecture and the structural patterns of rifted basins (e.g. Jackson and Vendeville, 1994; Rowan, 2014; Duretz et al., 2019; Jourdon et al., 2019,

2020). When the decoupling layer is pre-rift, it may act as a decollement layer leading to the partitioning of the deformation between the basement and overburden units during rifting (e.g. Jammes *et al*., 2010; Rowan, 2014; Ducoux et al., 2019; Coleman et al., 2019; Izquierdo-Llavall et al., 2020; Labaume & Teixell, 2020). During contractional deformation, pre-rift weak layers control the geometry of the thrust belt by favoring strain propagation toward the foreland thin-skinned tectonics (e.g. Letouzey *et al*., 1995; Jourdon et al., 2020).

The Pyrenean orogen (Fig. 1) results from the inversion and integration of a Lower Cretaceous hyperextended rift system with a pre-rift Triassic evaporitic layer (Lagabrielle and Bodinier, 2008; Jammes *et al*., 2009; Lagabrielle *et al*., 2010; Clerc *et al*., 2012, 2013; Clerc and Lagabrielle, 2014; Masini *et al*., 2014; Tugend *et al*., 2014; Lagabrielle *et al*., 2016; Clerc *et al*., 2016, Duretz et al., 2019; Jourdon et al., 2019, 2020). This crustal thinning episode was associated with a high-temperature and low-pressure (H*T*/L*P*) metamorphic event observed within narrow stripes on the south edge of North Pyrenean Zone (NPZ), forming the so-called Internal Metamorphic Zone (IMZ), where pre- to syn-rift sediments display a H*T*/L*P* metamorphism up to 600°C and below 4kbar (Bernus-Maury, 1984; Golberg and Leyreloup, 1990; Vauchez *et al*., 2013; Clerc *et al*., 2015). The NPZ domain is limited by major crustal faults, the North Pyrenean Frontal Thrust in the north and the North Pyrenean Fault along the southern rim, considered as a major discontinuity between two lithospheric plates and assumed to be active since the end of the Variscan orogenic cycle (Mattauer, 1968; Choukroune, 1976; Choukroune and Mattauer, 1978; Choukroune and ECORS Team, 1989).

Several studies investigated the tectonic evolution of Pyrenean belt and proposed estimates of the finite shortening based on N-S balanced geological sections (Choukroune and ECORS-Pyrenees Team, 1989; Roure et al., 1989; Muñoz, 1992; Teixell, 1998; Vergés et al., 2002; Martinez-Peña and Casas-Sainz, 2003; Beaumont et al., 2000; Mouthereau et al., 2014; Teixell et al., 2016; Ternois et al., 2019) but the role of decoupling layer and the early orogenic

processes were not assessed in details in these reconstructions. Only a few previous works described the early orogenic stages, suggesting the formation of an accretionary prism by the inversion of the former distal part of the rift system (Mouthereau et al., 2014; Ford et al., 2016). A recent study in the Western Pyrenees demonstrated that the early orogenic stage was associated with the inversion of the hyperextended rift system, reactivating rift-related extensional structures (Gomez-Romeu et al., 2019). In addition, the thick pre-rift Triassic evaporites, which had induced salt-tectonics during the Cretaceous rifting and gravity-driven post-rift deformation (e.g. Lopez-Mir et al., 2014; Saura et al., 2016; Teixell et al., 2016) acted as a decollement during the subsequent Pyrenean shortening (Canérot, 1988; Canérot et Lenoble, 1993; James & Canérot, 1999; Canérot, 2008; Ferrer *et al*., 2009 ; Jammes *et al*., 2009 ; 2010; Ducoux *et al*., 2019; Labaume & Teixell, 2020; Izquierdo-Llavall et al., 2020). The geometry of syn-rift structures is then difficult to assess because the former Cretaceous hyperextended rift basins were strongly overprinted by collisional deformation, except in the western and eastern Pyrenees. In particular, in the eastern Pyrenees, extension led to intense crustal boudinage and decoupling of the sedimentary cover from the basement (Clerc and Lagabrielle, 2014; Clerc *et al*., 2016). In this area, we have access to a complete section across basins which belonged to the former distal portion of the rift system, making this region a good candidate to study early orogenic processes corresponding to the inversion of the hyperextended rift basins.

By using new maximum temperature (T_{max}) reached by sedimentary rocks and structural data, the aim of this study is to reconsider the bulk structure of the NE portion of the eastern Pyrenees and investigate the role of a pre-rift weak evaporitic layer in the partitioning of the deformation during contractional deformation. In the eastern Pyrenees, published rift restorations suggest that the Agly massif was a high separating two basins (Vauchez et al., 2013; Clerc et al., 2015; 2016; Ternois et al., 2019; Odlum and Stockli, 2019); (1) the Boucheville basin sits on the rift

axis above exhumed lithospheric mantle, and (2) the Bas-Agly/St-Paul-de-Fenouillet basin sits on hyperthinned to thinned continental crust. This architecture is questionable, because it does not explain the H*T*/L*P* metamorphism observed in the present-day Bas-Agly syncline with temperatures similar to the Boucheville Basin, nor the low-temperature recorded in the St-Paul-de-Fenouillet syncline. We propose that the IMZ is allochthonous on top of the Agly North Pyrenean massif and its sedimentary cover and that the Bas-Agly syncline is a northern klippe of the IMZ. This interpretation suggests that the amount of Mesozoic sedimentary unit displacement in the eastern Pyrenees may be larger than classically proposed. In this work, we describe the succession of events that produce the present-day Pyrenean geometries, from the Late Cretaceous rifting stage to the Cenozoic main horizontal shortening, showing how the syn-rift geometry was reworked and how it controlled the finite structure of the belt.

2. Geological setting

2.1. The Pyrenean belt

The Pyrenean belt results from the collision between the Eurasian and Iberian plates from late Cretaceous to Miocene time. The present structure of the Pyrenean belt shows an asymmetric double-verging tectonic wedge above the northward underthrusting Iberian continental lithosphere (Choukroune and ECORS Team, 1989; Roure *et al*., 1989; Muñoz, 1992; Vergés *et al*., 1995; Teixell, 1998; Teixell *et al*., 2016; Chevrot et al., 2018). Across a maximum width of 150 km, the Pyrenees are traditionally divided into five distinct structural domains (Bertrand, 1940; Mattauer, 1968; Choukroune & Séguret, 1973; Castéras, 1974; Mattauer & Henry, 1974; Mirouse, 1980; Boillot, 1984) (Figure 1). (1) The Ebro and (2) the Aquitaine basins respectively correspond to the foreland and retro-foreland basins (e.g. Ford *et al*., 2016; Angrand et al., 2018). (3) The NPZ is a WNW-ESE elongated ribbon made of thrusts and folds deforming the Mesozoic sedimentary succession of Cretaceous basins and locally associated with basement blocks (North Pyrenean massifs). The NPZ is limited by the North Pyrenean Frontal Thrust

(NPFT) and the North Pyrenean Fault. (4) The Axial Zone, the topographic backbone of the Pyrenees, is mainly composed of Paleozoic rocks deformed during the Variscan and Alpine orogenic cycles (Mattauer, 1964; Mattauer and Seguret, 1966; Debat, 1969). Finally, (5) the South Pyrenean Zone (SPZ) consists of Mesozoic to Eocene sedimentary rocks transported southward over the Ebro basin above the South Pyrenean Frontal Thrust (SPFT) localized within the Triassic evaporites (Séguret, 1972; Vergés and Muñoz, 1990; López-Mir *et al*., 2014).

The architecture of the Pyrenees results from the inversion and integration in the orogen of early Aptian to early Cenomanian rifted basins (Lagabrielle and Bodinier, 2008; Jammes *et al*., 2009, 2010; Lagabrielle *et al*., 2010; Clerc *et al*., 2012, 2013; Masini *et al*., 2014; Tugend *et al*., 2014; Lagabrielle *et al*., 2016). Rifting has then evolved to hyperextension and mantle exhumation in the NPZ and the Basque-Cantabrian Basin as suggested by several mantle exposures, then to drifting further west in the Bay of Biscay (e.g. Fabries *et al*., 1991, 1998; Lagabrielle and Bodinier, 2008; Jammes *et al*., 2009; Clerc *et al*., 2012, 2013; Masini *et al*., 2014; Tugend *et al*., 2014; Lagabrielle *et al*., 2016). It is commonly accepted that hyperextension and mantle exhumation are responsible for a high-temperature and low-pressure (H*T*/L*P*) metamorphism (Ravier, 1959; Bernus-Maury, 1984; Azambre and Rossy, 1976; Golberg and Leyreloup, 1990; Dauteuil and Ricou, 1989; Clerc and Lagabrielle, 2014; Clerc *et al*., 2015; Ducoux, 2017; Ducoux *et al*., 2019). This H*T*/L*P* metamorphic event affecting the southern NPZ it is mainly evidenced by marbles of the IMZ issued from pre-rift to syn-rift sediments, with peak conditions up to 600°C and below 4kbar (Bernus-Maury, 1984; Golberg and Leyreloup, 1990; Vauchez *et al*., 2013; Clerc *et al*., 2015). Available T_{max}, obtained with the Raman Spectroscopy of Carbonaceous Materials (RSCM) method along the IMZ, first suggested the existence of a temperature gradient from west to east (Clerc *et al*. 2015), but more recent studies of the westernmost orogen (i.e. Basque-Cantabrian Basin) showed otherwise with equally high

maximum temperatures in the east and west (Ducoux *et al*., 2019). Published geochronological data indicate ages ranging from Albian to Santonian (110–85 Ma) for this H*T*/L*P* metamorphic event, demonstrating a short delay (10 My) between the end of rifting event (Cenomanian) and the end of the H*T*/L*P* metamorphism (Santonian) (Albarède and Michard-Vitrac, 1978a; Albarède and Michard-Vitrac, 1978b; Montigny *et al*., 1986; Golberg and Maluski, 1988; Golberg *et al*., 1986; Bandet and Gourinard in Thiébaut *et al*., 1988; Clerc *et al*., 2015; Chelalou *et al*., 2016).

The end of rifting was rapidly followed by the onset of convergence across the Pyrenean belt during the Late Santonian, as suggested by tectonic and sedimentological data (Garrido-Megias & Rios 1972; Muñoz, 1992; Vergés *et al*., 1995; Teixell, 1998; Vergés & García-Senz, 2001; García-Senz 2002; McClay *et al*., 2004; Biteau *et al*., 2006; Mouthereau *et al*., 2014). After a quiet tectonic period during the Paleocene (Danian to early Selandian, Ford *et al*., 2016), the main collisional phase occurred in Eocene-Oligocene times (Muñoz 1992, 2002; Vergès *et al*. 2002; Mouthereau *et al*., 2014), ultimately leading to the present-day structure. The collisional phase ended during the Chattian in the NPZ (Ortiz et al., 2020) but remained active in the southern Pyrenees until the early Miocene (Muñoz et al., 1992; Hogan and Burbank, 1996; Teixell, 1996; Millán Garrido et al., 2000; Millán Garrido, 2006; Jolivet et al., 2007; Oliva-Urcia et al., 2015; Labaume et al., 2016). Finally, after the main collisional event, since the middle Oligocene, the Eastern Pyrenees were affected by extensional deformation associated with the opening of the Valencia Trough and Gulf of Lion (e.g. Gorini et al., 1993; Gorini et al., 1994; Mauffret et al., 1995; 2001; Roca *et al*., 1999; Vergés and Garcia-Senz, 2001; Roca, 2001; Wehr et al., 2018; Etheve *et al*., 2018; Jolivet et al., 2020).

2.2. The eastern North Pyrenean Zone

The architecture of the eastern NPZ consists of the Agly Massif, the easternmost North Pyrenean massif (Fig. 1), bounded by the Boucheville Basin to the south and the St-Paul-de-Fenouillet and Bas-Agly synclines to the north (Fig. 2). The Agly massif, which represents a condensed crustal section, is composed of plutonic and metamorphic rocks affected by a Variscan H*T*/L*P* metamorphism (granulite to greenschist facies) (Barnolas *et al*., 1996; Guille *et al*., 2018; Olivier *et al*., 2008; Wickham & Oxburgh, 1986). This metamorphic event is characterized by a strong geothermal gradient, locally higher than 100°C/km (Fonteilles 1976; Vielzeuf 1984; Delay 1990, Berger et al., 1993). The upper parts of the massif are composed by thick Ediacarian to Devonian metasediments and by granitoids (Fonteilles, 1970; Berger *et al*., 1993; Casas and Palacios, 2012). The deepest parts contain thin sheets of paragneisses and orthogneisses derived from granitic sills emplaced at ca. 540 Ma (Guille *et al*., 2019). Deformation and late Variscan H*T*/L*P* metamorphism that affect these para and ortho-derived series have been variably interpreted as distributed mylonitic shear zones during the Variscan orogeny between 305 and 296 Ma (e.g Olivier *et al*., 2004, 2008; Wickham & Oxburgh, 1986; Vanardois et al., 2020) or during a late Variscan extensional event related to a major detachment fault in the middle crust (Bouhalier *et al*., 1991). Part of this high-strain mylonitic deformation has alternatively been attributed to the Cretaceous rifting event (Passchier, 1984; Costa and Maluski, 1988; St Blanquat *et al*., 1990; Delay, 1990; Delay & Paquet, 1989; Paquet and Mansy, 1991; Vauchez *et al*., 2013; Clerc *et al*., 2016; Odlum and Stockli, 2019). Low-grade Ordovician to Devonian metasediments (mainly metapelites, shales and carbonates) compose the northeastern part of the Agly massif. They were weakly metamorphosed in the chlorite zone of the regional H*T*/L*P* metamorphism (Berger et al., 1993), while high-grade gneissic and granulitic rocks are observed in the southwestern domain (Fig. 2). The Agly basement was also affected by hydrothermal alteration during the rifting episode, as revealed by 98±2 Ma albitization within the St. Arnac pluton (Poujol *et al*., 2010). This massif is finally crosscut by

numerous N110°E-striking faults displaying down-dip slickenlines attributed to Pyrenean collision (Olivier *et al*., 2004).

The Mesozoic sedimentary sequence of the area is exposed in the St-Paul-de-Fenouillet and Bas-Agly synclines, and in the Boucheville basin. It starts with unconformable continental Permian to Middle Triassic deposits, only observed in the southern margin of the Mouthoumet massif. These sediments are missing over the Agly massif and the northern margin of the Axial Zone (Fig. 2). Shallow marine Upper Triassic sediments are carbonates, clays and evaporites (Keuper facies) passing upward to Liassic to late Aptian shallow marine limestones. The Albian period is then marked by the opening of the large and interconnected basins Albian to Cenomanian "Flysch Noir" basin (Debroas & Souquet 1976; Debroas, 1990; Berger *et al*., 1997), later dismembered during convergence and now preserved in the St-Paul-de-Fenouillet, Boucheville and Bas-Agly synclines (Fig. 2). Post-rift late Cenomanian-Turonian flysch deposits are transgressive on underlying older syn-rift sequences (Debroas 1990; Debroas in Ternet *et al*., 1997), and were continuously deposited until the early-Coniacian, onlapping the northern part of Axial Zone and the North Pyrenean massifs (Debroas, 1987; 1990). The Pyrenean convergence was responsible for the positive inversion of the rifted basins from the Santonian to the Eocene (Bessière *et al*., 1989). From Miocene to Present, the eastern part of the Pyrenean range was characterized by the development of extensional structures due to the opening of the Gulf of Lion (Berger *et al*., 1993).

The Boucheville unit is a large synclinorium (Choukroune, 1970, Chelalou *et al*., 2016) showing evidence of early extensional ductile deformation coeval with the rifting event (Chelalou *et al*., 2016). The Boucheville syncline and the eastern part of the Agly massif are separated from the Axial Zone by the sub-vertical North Pyrenean Fault (Fig. 2). To the northeast of the Agly massif, the Bas-Agly syncline overthrusts the eastern part of the St-Paul-de-Fenouillet syncline (Fig. 2) that is limited, to the north, by the south-dipping NPFT (Fig. 2).

The northern border of the Agly massif, corresponding to the southern Bas-Agly syncline, shows the remains of a décollement of the pre-rift cover (Durand-Delga, 1964; Légier *et al*., 1987; Clerc and Lagabrielle, 2014; Clerc *et al*., 2016) with tectonic lineations and drag folds indicating a top to the NNE displacement (Légier *et al*., 1987; Vauchez *et al*., 2013). The Bas-Agly/St-Paul-de-Fenouillet and the Boucheville synclines are interpreted in most restorations, as two separate rifted basins on either side of the Agly massif, the latter corresponding to a tilted basement block (Vauchez et al., 2013; Clerc et al., 2015; 2016; Ternois et al., 2019; Odlum and Stockli, 2019). In these rift restorations, the Boucheville syncline sits on the rift axis above exhumed lithospheric mantle, while the Bas-Agly and St-Paul-de-Fenouillet synclines sit on hyperthinned to thinned continental crust.

3. Materials and Methods

To determine the distribution of the H*T*/L*P* metamorphism and then compare with the deformation pattern, we sampled 9 Mesozoic rocks of the Bas-Agly and the St-Paul-de-Fenouillet synclines for determining the maximum recorded temperatures with the RSCM method (Beyssac *et al*. 2002a; Lafhid *et al*. 2010). This data set completes the previous works focused on the H*T*/L*P* metamorphism (Clerc *et al*., 2015; Chelalou, 2015). This analytical method allows characterizing the structural evolution of carbonaceous material (CM), reflecting a transformation from disordered to well-ordered CM during metamorphism (Wopenka and Pasteris, 1993). The relation of this increasing graphitization with temperature was quantified, leading to a tool to determine peak temperatures attained by metamorphic rocks (Beyssac *et al*., 2002a). Since graphitization is an irreversible process, the RSCM method gives the temperature peak (Pasteris and Wopenka, 1991; Beyssac *et al*., 2002a). This is the basis of the RSCM geothermometer, which was calibrated in the range between 330 and 650°C by Beyssac *et al*. (2002a) and extended to the range between 200 and 320°C by Lahfid *et al*. (2010). In this study, we applied these two calibrations to estimate paleotemperatures in carbonates and pelitic

metasedimentary rocks from the Paleozoic and Upper Cretaceous series of the study area. Raman analysis protocol is described in supplementary material. The entire results are presented in Table SM1 in supplementary materials and Figures 2 and 3 (T_{max} values of this study are display in red) with the details of the data acquisition protocol.

4. Thermal pattern of the eastern NPZ

4.1. Distribution of the H*T*/L*P* metamorphism

The eastern part of NPZ has been extensively studied and numerous studies propose temperature estimates for the H*T*/L*P* Pyrenean metamorphic event with different methods including the RSCM approach (e.g Golberg, 1987; Golberg and Leyreloup, 1990; Clerc *et al*., 2015; Chelalou, 2015; Chelalou *et al*., 2016). The Boucheville syncline is largely affected by this H*T*/L*P* metamorphism and has recorded rather homogeneous peak temperatures comprised between 530 and 580°C (Golberg et Leyreloup, 1990; Chelalou *et al*., 2016) (Figs. 2 and 3). Locally, near the southern edge of the basin, within pre-rift Jurassic sediments, T_{max} are below 500°C (Chelalou *et al*., 2016). According to Clerc et al. (2015), the eastern part of the Agly massif, made of Ordovician to Devonian metasediments, experienced T_{max} 351±3°C measured in Silurian metasediments and close to the contact with the south margin of the Bas-Agly syncline (Fig. 2). Our data confirm this trend, with a T_{max} of 351±12°C measured a few kilometers westward. This range of T_{max} shows that the thermal event has not affected or has not exceeded 350°C in the upper part of the Agly massif.

Remnants of the metamorphic Mesozoic cover lying on the central-western part of Agly basement (Berger *et al*., 1993; Fonteilles *et al*., 1993), more precisely in the Serres de Verges area, correspond to Jurassic and Lower Cretaceous brecciated metasediments. We measured in this unit a T_{max} of 424± 32°C obtained in foliated clasts (Fig. 2). This value of T_{max} shows high-grade metamorphic conditions of the Mesozoic sedimentary cover, located above high-grade

Variscan metamorphic rocks of the Agly massif. Thus, there is no observed metamorphic gap between the breccia and the basement. Measured T_{max} in the Mesozoic metasediments of the eastern Agly massif are instead higher than in Paleozoic rocks, the latter being only affected by low-grade metamorphism under low greenschist-facies conditions.

We measured T_{max} higher than 550°C in the Cretaceous core of the Bas-Agly syncline. The highest T_{max} estimated in this syncline correspond to respectively 570 ± 27°C and 566 ± 15°C in Valanginian and Aptian metacarbonates. A T_{max} of 534 ± 19°C is recorded in black Albian marbles in the central part of the syncline (Fig. 2). In a previous study (Chelalou, 2015), a similar range of T_{max} comprise between 530 to 559°C was characterized. In the southern Bas-Agly syncline, close to the contact with the Agly massif and documented by previous studies, T_{max} decreases around 350°C with a local value of 494°C ± 7°C in anhydrite-rich Upper Triassic sediments (Clerc et al., 2015). Intermediate temperatures comprised between 450 and 400°C (Golberg and Leyreloup, 1990) indicate a progressive southward decrease of metamorphic grade (Fig. 2). In the Bas-Agly, the highest temperatures are thus recorded in the central part of the syncline.

In the Albian marls of the St-Paul-de-Fenouillet syncline, we measured a local T_{max} value of 246°C and two T_{max} lower than 200°C. These temperatures corresponding to low-grade metamorphism, are in agreement with previous data obtained in this syncline, which are comprised between 200 and 290°C (Chelalou *et al*., 2016). In the eastern part of this basin, close to the contact with the Bas-Agly syncline, we also obtained T_{max} lower than 200°C (Fig. 2) confirming that the whole basin has not been heated, which marks a major difference with both the Bas-Agly and Boucheville synclines.

A map of Cretaceous H*T*/L*P* metamorphism distribution has been interpolated from the available T_{max} and field geological data in the eastern part of the ZNP (Fig. 3). It shows a clear

thermal contrast between the Boucheville and the Bas-Agly synclines on the one hand, and the St-Paul-de-Fenouillet syncline on the other hand. Both the Bas-Agly and Boucheville synclines show lateral temperature gradients within the sediments that cannot be attributed to differential burial. Actually, the highest temperatures are observed in the syn-rift sediments, while pre-rift sediments experienced only moderate temperatures (~400°C for the Boucheville syncline and between 350 and 400°C for Bas-Agly syncline) (Fig. 3). Consequently, H*T*/L*P* metamorphic isograds are oblique on the bedding in those basins and on different structures observed in this area. A thermal gap (>250°C) is observed across the Tautavel thrust fault bounding the Bas-Agly and St-Paul-de-Fenouillet synclines, connecting northward with the NPFT (Figs. 2 and 3).

To summarize the distribution of the thermal imprint of the Cretaceous H*T*/L*P* metamorphism, the Boucheville and Bas-Agly synclines show the highest grade of metamorphism with T_{max} exceeding 500°C. The underlying eastern Agly massif experienced T_{max} never exceeding 350°C, a peak-temperature colder than these two metamorphic Mesozoic synclines. Furthermore, this contrast of T_{max} between basement and metamorphic Mesozoic sedimentary cover is attested by remnants of Mesozoic sediments located above the Agly massif, where T_{max} exceeds 400°C. Thermal contrast is most significant between the Boucheville/Bas-Agly-synclines and the St-Paul-de-Fenouillet syncline where T_{max} does not exceed 250°C.

4.2. Deformation of basement versus Mesozoic sedimentary cover

Below the basal contact of the Bas-Agly syncline, the north-eastern margin of the Agly massif is made of low metamorphic grade sediments (Fig. 4). Silurian sandstones and feldspathic shales that composed the Paleozoic basement of the northeastern Agly massif still show graptolites and preserved turbiditic sedimentary figures. This upper part of the basement is only affected by a series of N110°E localized metric-scale shear bands (Fig. 5), some of which corresponding to N-verging normal faults (Fig. 5a). We also observe reverse faults with a top-

to-the S sense of shear, suggested by folding and reverse offset of sandstone layers (Fig. 5b). The northeast Agly massif is thus affected by various brittle and brittle-ductile shears, but no pervasive ductile deformation is observed (Fig. 5), in agreement with the measured low T_{max}. Our observations are in agreement with previous studies (Légier *et al*., 1987; Vauchez *et al*., 2013). Only the contact between low-grade metasediments and high-grade metamorphic rocks underneath are associated with ductile deformation previously attributed to the Variscan event (Berger et al., 1933 and references therein).

In contrast with the Paleozoic low-grade metasediments of the Agly Massif affected by brittle deformation, the Rhaetian and Liassic sediments of the Bas-Agly syncline show an intense ductile deformation with stretching lineation and plurimetric-scale boudinage (Figs. 4 and 6), with a NNE-ward sense of shear (Vauchez et al., 2013). The base of this sedimentary cover is associated to the development of north-verging recumbent metric folds as well (Fig. 6a and b). It is worth noting the presence of Upper Triassic evaporites at the base of the sedimentary pile. The contrasted deformation observed in the different units confirmed the distribution of T_{max} with higher temperature in the cover than in the basement.

As for the Bas-Agly, this ductile deformation is also observed in the Boucheville syncline equally affected by the H*T*/L*P* metamorphism. This syncline is strongly overprinted by Pyrenean-related compressional deformation responsible for the development of N110°-striking cleavage (Fig. 4). This cleavage is coeval with the development of the main faults (as the North Pyrenean Fault) which bound the Boucheville syncline, attributed to the late convergence (Berger et al., 1993). Concerning the Bas-Agly syncline, only its southern margin is folded and associated to the late subvertical cleavage. This deformation zone is located along the extension of the Latour-de-France Fault, responsible of the late thrusting of the Agly massif over the Bas-Agly. This cleavage is not clearly expressed in the rest of the Bas-Agly syncline. However, this subvertical cleavage extends into the St-Paul-de-Fenouillet syncline until the

NPFT (Fig. 4). No cleavage is observed to the north of the North Pyrenean Frontal Thrust. Only salt tectonics-related structure is preserved (Fig. 4).

The contact between the Mesozoic sediments and the crystalline/metamorphic basement (orange faults in Fig. 4) is mainly observed in the eastern Boucheville syncline and along the southern margin of the Bas-Agly syncline. This flat-lying contact is characterized by the presence of breccia recognized on the top of the Agly Massif and at the base of Jurassic series in the Bas-Agly. Furthermore, the surface of this contact is subsequently deformed and truncated by a fault (Durand-Delga, 1964). The contact between the Bas-Agly and the St-Paul-de-Fenouillet corresponds to the Tautavel fault which consist to a low angle thrust connected to the NPFT (Fig. 4).

The Boucheville and Bas-Agly syncline are always limited by tectonic contacts with the basement. On the opposite, the St-Paul-de-Fenouillet syncline is lying over the northern margin of the Agly massif without any significant deformation (Fig. 4), suggesting that it could be the autochthonous Mesozoic sedimentary cover of the Agly massif.

5. Discussion and interpretation: tectonic consequences of the IMZ thermal structure

5.1. Architecture of the eastern North Pyrenean Zone

The geological cross-sections of figure 7 show the structure of the eastern part of the IMZ and its relationships with NPZ and the Agly massif (Fig. 7). The Boucheville Basin corresponds to an asymmetric synclinorium (e.g. Choukroune, 1976; Chelalou *et al*., 2016) bounded by two steeply-dipping major faults, including the North Pyrenean Fault to the south. These faults affect both the basement and the IMZ (Figs. 4 and 7a) and can be extended eastward within the Agly massif where they offset Variscan metamorphic isograds (Fig. 7a). These steeply-dipping faults are intersected by late normal faults linked to the formation of grabens filled by Miocene-

Quaternary sediments (Figs. 4 and 7b). Variscan structures within the Agly massif have been deformed during the Pyrenean compression, and are affected by WNW-ESE striking reverse faults (Olivier *et al*., 2004).

West of Latour-de-France, the contact between the Bas-Agly syncline and the Agly massif is overturned and faulted (Latour-de-France Fault) while, further east, the Bas-Agly cover is flat-lying on the top of Paleozoic series with a tectonic contact (Figs. 2 and 4). The northern limb of the Bas-Agly syncline overthrusts the St-Paul-de-Fenouillet syncline through the Tautavel Fault that extends and connects with the NPFT further north (Fig. 4). West of Maury, the low-temperature Mesozoic sequence of the St-Paul-de-Fenouillet syncline, which is the cover of the Paleozoic basement of the Agly massif, is still present, only partly detached thanks to the Triassic evaporites.

Isograds of metamorphism are represented on the geological cross sections and show the distribution of H*T*/L*P* Cretaceous metamorphism in the eastern NPZ (Fig. 7). In the Boucheville Basin, temperature isograds are clearly intersected by steeply-dipping faults that bound the basin (Fig. 7a). Moreover, a large gap of temperature across the Tautavel Fault is evidenced on both cross sections (Fig. 7). Folding observed in the Mesozoic sedimentary cover results partly from the late compressional event, but some folds may result from the halokinesis active during the rifting event. Temperature isograds are overturned, intersected and shifted by late deformational structures and faults. However, the distribution of metamorphism in these synclines is rather heterogenous and shows lateral temperature gradients within the basin. Isograds in the Bas-Agly syncline clearly intersect bedding. This observation was already made in the Western Pyrenees, especially in the Basque-Cantabrian Basin and in the Chaînons Béarnais area, where the obliquity of isotherms on the structure is due to a pre-metamorphic folding related to salt tectonics (Ducoux *et al*. 2019; Izquierdo-Llavall *et al*., 2020).

5.2. Significance of temperature and deformation contrasts across tectonic contacts.

The central parts of the Bas-Agly and Boucheville synclines show significantly higher temperature >450°C, while the St-Paul-de-Fenouillet syncline shows temperatures <250°C. The temperature gap between the Bas-Agly and St-Paul-de-Fenouillet synclines is abrupt and corresponds to the Tautavel thrust fault. On the other hand, the metamorphic contrast is significant between Paleozoic shales with low-grade greenschist facies conditions (H*T*/L*P* Variscan metamorphism) of the northern Agly massif and Mesozoic sediments with higher T_{max}. Consequently, the Bas-Agly and Boucheville synclines were affected by Cretaceous H*T*-metamorphism, coeval with mantle exhumation, but not the overlying northern Agly massif which never experienced temperature exceeding 350°C. T_{max} measured in the Paleozoic metasediments of the northern Agly massif can either date back to the Paleozoic or to the Cretaceous rifting event, but the measured temperature shows that the basement has seen lower temperatures than the overlying cover. Note that we do not discuss here the southern part of the Agly massif where the H*T*/L*P* metamorphism has been attributed to the Variscan event (Vielzeuf and Kornprobst, 1984) or to the Cretaceous HT/LP episode (Odlum and Stockli, 2019). It is commonly admitted that the regional H*T*/L*P* that affects the NPZ is coeval with the Lower Cretaceous crustal thinning event (Ravier, 1959; Bernus-Maury, 1984; Azambre and Rossy, 1976; Golberg and Leyreloup, 1990; Dauteuil and Ricou, 1989; Clerc and Lagabrielle, 2014; Clerc *et al*., 2015). In the Boucheville synclinorium, the paleogeothermal gradient during this H*T*/L*P* metamorphic event has been estimated between 70 and 80°C/km (Chelalou *et al*., 2016). Recent low-temperature thermochronological study indicates that the Agly block cooled below 250°C during the syn- to post rifting (117-90 Ma) (Odlum & Stockli, 2019; Ternois *et al*., 2019), indicating significant lower temperatures than bounding metamorphic sedimentary basins that recorded temperatures >500°C during the post-rift period (95-90 Ma) (Clerc et al.,

2015) . Thus, the H*T*/L*P* metamorphism during the Cretaceous would have been confined to the southern Agly massif, like further west in the Aulus Basin for instance.

With reference to the distribution of H*T*-metamorphism, the deformation in the different units is also contrasted. Intense ductile deformation is observed in the Bas-Agly and Boucheville synclines that recorded the highest temperatures, while the underlying Silurian strata corresponding to Paleozoic cover of the Agly Massif, where temperature are lower, are much less deformed and certainly not mylonitized. Remnants of a Mesozoic cover are locally preserved on top of the Agly Massif, such as cataclastic breccias containing clasts of H*T* ductilely deformed marbles sealed by unmetamorphic cement. These observations and the temperature higher than 400°C in marble clasts in the Serre de Vergés area confirm that the breccia is a post-metamorphic event.

In previous studies, the contact between the Agly massif and the Bas-Agly syncline has been interpreted as the result of basal truncation of a detached Mesozoic cover (Durand-Delga, 1964; Légier *et al*., 1987) and recently reinterpreted as a north-dipping extensional detachment, the Agly massif being in the position of a metamorphic core complex (Vauchez *et al*., 2013; Clerc and Lagabrielle, 2014) where extensional deformation near the contact in the Mesozoic cover would be expressed by the boudinage and drag folds (Clerc *et al*., 2016). In this interpretation, the Bas-Agly syncline corresponds to the detached sedimentary cover of the Agly massif, decoupled via a décollement layer in Upper Triassic sediments (Vauchez *et al*., 2013; Clerc *et al*., 2016). EBSD and field study in carbonate layers of the base of the Bas-Agly syncline suggest that this N- to NE trending ductile shearing was developed at a temperature around 400°C (Vauchez *et al*., 2013). In the opposite way, a recent study suggests that the Lower Cretaceous exhumation of the southern part of the Agly massif by extension was accommodated by a top-to-the south detachment (Odlum & Stockli, 2019).

The extensional model and the pre-orogenic restorations of Vauchez *et al* (2013), Clerc *et al*. (2016) and more recently the crustal-scale model of Ternois *et al*. (2019) and Odlum & Stockli (2019) do not easily explain the thermal imprint measured in the central part of the Bas-Agly syncline. In particular they do not explain the higher T_{max} measured in the Bas-Agly syncline. Figure 8 shows two typical situations of a metamorphic core complex and a thrust in terms of deformation and thermal structure. First of all the contrast in T_{max} is the opposite in the two situations. A detachment with a significant displacement will inevitably lead to cold (superficial) over hot (deep) units, while a thrust will show the opposite arrangement (Fig. 8a). Then, all detachments show a continuum of ductile-to-brittle deformation within a distinct shear zone that is mostly observed in the lower plate, below the detachment (Crittenden *et al*., 1980; Davis and Lister, 1988) and the lower plate display more ductile deformation while the upper plate shows mostly brittle deformation, which is the exact opposite to what is observed in the study area. The deformation observed in the Paleozoic sediments of the top of the Agly massif is weak and certainly does not correspond to a major shear zone.

Then the question arises about the significance of the observed ductile deformation at the base of the Bas-Agly syncline. The N-NE trend of stretching lineations and calcite fabrics near the base of the Bas-Agly syncline described by Vauchez *et al*. (2013) attests for a northward displacement of the metamorphic unit corresponding to the current Bas-Agly syncline, but it does not prove that it corresponds to an extensional deformation. Here, the large thermal contrast between the hot metamorphic Mesozoic cover and the colder Paleozoic basement underneath is opposite and thus more compatible with a thrust than a detachment (Fig. 8b).

Finally, models proposed by Vauchez *et al* (2013), Clerc *et al*. (2016), Ternois *et al*. (2019) and Odlum & Stockli (2019) describe the Boucheville and Bas-Agly synclines as two narrow disconnected basins on either side of the Agly basement massif, but this assumption conflicts with sedimentological observations indicating that Aptian, Albian and Lower Cretaceous

pelagic sediments (corresponding to "Flysch noirs") were likely deposited in a unique large basin and not in two narrow separated basins (Olivier, 2013).

The main question then concerns the link between the Mesozoic sedimentary cover and Paleozoic rocks of the Agly massif. A section along the northern margin of the Agly massif further west, near Maury, shows that the St-Paul-de-Fenouillet syncline is the poorly metamorphosed Mesozoic cover of the Agly Paleozoic basement, in agreement with the low temperatures observed in the St-Paul-de-Fenouillet Basin. When moving east, this sedimentary cover is substituted by the Bas-Agly syncline that is more intensely metamorphosed and the contact between the St-Paul-de-Fenouillet syncline and the Bas-Agly corresponds to a well-characterized thrust that connects to the north with the North Pyrenean Frontal thrust. Then, two hypotheses can be proposed: (1) the Bas-Agly syncline may be the eastern equivalent of the St-Paul-de-Fenouillet Basin with a higher metamorphic grade and the two basins were carried along the basal decollement in Upper Triassic evaporites until they got into close contact; (2) alternatively, the Bas-Agly syncline may be the western termination of a rift segment developing eastward, if we consider the eastern termination of Pyrenees as a relay or accommodation zone where the rift axes are shifted. The Boucheville and Bas-Agly synclines may corresponded to V-shaped terminations of two rifted basins, as the western Pyrenees for instance (e.g. Lescoutre & Manatschal, 2020); (3) the Bas-Agly syncline is not the cover of the Agly massif and corresponds instead to a displaced outlier of a more internal and hotter unit where high temperature is due to mantle exhumation as elsewhere in the NPZ.

By combining structural observations and new T_{max} dataset we then propose an alternative interpretation whereby the Bas-Agly syncline corresponds to a northern klippe of the Boucheville Basin thrusted over the Agly massif and a part of St-Paul-de-Fenouillet during the Pyrenean shortening. In this interpretation, the Bas-Agly would connect above the Agly massif with the more internal Boucheville syncline, where high temperatures are recorded.

The top-north detachment described by Vauchez et al. (2013) in the northeastern part of the Agly Massif in then reinterpreted as a top-to-the north thrust instead, assisted by regional-scale well known Upper Triassic evaporites layer. This interpretation explains the distribution of metamorphism, the observed temperature contrasts recorded within the different synclines and the distribution of deformation.

5.3 A 2D crustal-scale geodynamic model

Figure 9 presents a basin-scale restoration model showing a possible evolution of the eastern end of the NPZ from the rifting stage to the end of the Pyrenean orogeny. Based on the model of Ternois *et al*. (2019) for the crustal architecture, we propose a different interpretation for the sedimentary cover, in which the Bas-Agly syncline represents an allochthonous unit initially connected with the Boucheville syncline above a body of exhumed mantle during the Cretaceous rifting, where both formed a single basin and then transported northward by a thrust.

The first step represents the rift template before the onset of the convergence during the Santonian with the inversion of the hyperextended rifted margins formed a span of 30 Myrs between early Aptian to early Cenomanian stages (Fig. 9a). Rifting was associated to hyperthinning of the lithosphere accommodated by the development of a large-scale top-to-the-south detachment fault located at the base of the basin which induced mantle exhumation and H*T*/L*P* metamorphism in the pre- and syn-rift sediments. Such model of crustal boudinage was already proposed by Clerc *et al*. (2016), but we show here that the northern side of the Agly massif was not affected by ductile deformation during rifting. On the opposite, the Cretaceous basin was affected by intense ductile deformation during this episode, especially in the northern part of the Boucheville Basin (Chelalou *et al*., 2016). The syn-rift geometry supposes that the Boucheville, Bas-Agly and St-Paul-de-Fenouillet basins are connected and are filled mainly by Albian-Cenomanian deposits. The Agly massif represents a paleo-topographic high, but it was never significantly eroded before the Late Cretaceous, because there is no evidence of Paleozoic

clasts in Aptian to Cenomanian deposits (Olivier *et al*., 2013). It is only covered by a thin succession of syn-rift sediment (Fig. 9a). We suggest that the Agly massif separates two basins probably interconnected laterally farther west and probably farther east. There is no argument to bury the Agly paleo-high beneath a thick pile of syn-rift sediments. On the contrary, there is a possibility that this paleo-high was only buried beneath post-rift successions. This assumption is supported by recent thermochronological data (Odlum & Stockli, 2019; Ternois *et al*., 2019). The eastern NPZ consist in rift and salt architecture with salt pillows, diapirs and raft of the syn-rift sediment further north, driven by gravity gliding of the Mesozoic cover. In this model, syn-rift sediments were deposited over the pre-rift sediments that experienced gravity gliding and were juxtaposed above exhumed mantle and a thin continental crust corresponding to the future Boucheville and Bas-Agly basins where H*T*/L*P* metamorphism developed (Fig. 9a). We assume a juxtaposition of pre- and syn-rift sediments and exhumed mantle; but we cannot exclude the possibility that the Mesozoic basin was sitting on a very thin continental crust and not directly on the exhumed mantle, because there is no evidence of mantle clast and/or volcanism in this area. During the onset of convergence, the hyperextended domain is firstly reactivated and inverted up to collision of both margins Gómez-Romeu *et al*. (2019).

The second step corresponds to the Late Cretaceous convergence with the inversion of the two hyper-extended margins after underthrusting of the exhumed mantle and reactivation of the necking domain associated to the development of the south-verging thrusts located in the Axial Zone and the NPFT (Fig. 9b). A major thin-skinned flat-lying thrust rooted in the Upper Triassic decollement level allowed the northward displacement of the metamorphic part of the basin on top of the St-Paul-de-Fenouillet Basin that recorded only low-grade metamorphism. We hypothesize that the inherited detachment at the base of the basin associated to the decollement layer has been reactivated as a thrust. Early salt pillows and diapirs could be responsible for the localization of the major thin-skinned thrust, corresponding to the current Tautavel fault. In

addition, this thrust is probably responsible for the development of breccias at the base of the pre-rift cover. Indeed, these breccias may be a witness of the decollement level localized between the basement and the Mesozoic sedimentary cover (Clerc *et al*., 2016). It is more difficult to estimate the amount and the direction of this general displacement. The displacement and the thermal contrast seem to decrease toward the east, and Bas-Agly syncline seems to be interconnected with the St-Paul-de-Fenouillet syncline. It may be possible that the deformation softened eastward, especially as this area corresponding to a well-known transfer zone corresponding to the Corbières virgation (Tugend et al., 2014). In the rest of the Pyrenees, the IMZ where higher T_{max} are recorded, is always interconnected with non-metamorphic basins to the north where North Pyrenean massifs are missing or not outcropping (Clerc et al., 2015). Recent study indicates that the thermal imprint of the metamorphism gently decreases when moving away from the former distal part of the rift system (Ducoux et al., 2019).

The Paleocene corresponds to a period of tectonic quiescence, the convergence rate strongly decreasing (Desegaulx and Brunet, 1990; Ford *et al*., 2016; Rougier *et al*., 2016; Machiavelli *et al*., 2017; Grool *et al*., 2018; Dielforder *et al*., 2019; Ternois *et al*., 2019), as emphasized by the absence of cooling at that age in the Agly blocks (Ternois *et al*., 2019) and by a minimal deposition of clastic sediments in the Aquitaine retro-foreland basin (Desegaulx and Brunet, 1990, Ford *et al*., 2016). This tectonic quiescence could be attributed to the transition period between the closure and inversion of both hyperextended domain and the beginning of crustal thickening related to the collision strictly speaking.

The third step corresponds to the onset of the main collision phase and the beginning of crustal thickening involving thick-skinned tectonic style and the development of crustal-scale thrust faults in the pro-wedge domain (Ternois *et al*., 2019) (Fig. 9c). A major part of the deformation is then accommodated within the basement by the reactivation of former normal faults in the retro-wedge and by the neoformation of thrusts in the pro-wedge. The progressive crustal

thickening is responsible for basement exhumation, especially the Agly massif and sedimentary cover as well (Fig. 9c). Recent thermochronological data indeed indicate a rapid exhumation of the Agly massif near the surface during the Eocene, while the NPZ continues to shorten and deformation migrates northward (Ternois *et al*., 2019). These recent data are in agreement with other published thermochronological data which consistently suggest such a timing: 49±4 to 35±3 Ma in Mauléon Basin (Western Pyrenees) (Vacherat *et al*., 2014); 50 to 35 Ma for North Pyrenean massifs in the central Pyrenees (Vacherat *et al*., 2016); 44 to 35 Ma in the Axial Zone (Fitzgerald *et al*., 1999). In our model, the exhumation of the Agly block along the main thrust caused a shift of the primary thrust (i.e. Tautavel fault, Figs. 2, 4 and 6), and a folding of the Mesozoic cover that generated the current shape of the Bas-Agly syncline.

The last step corresponds to the end of collision with nappe stacking of the Axial Zone (Fig. 9d). The shortening is mainly localized on the future SPFT at depth and on the NPFT. From the middle Eocene to the early Oligocene, the Axial Zone records higher exhumation rates (Whitchurch *et al*., 2011; Rushlow *et al*., 2013; Mouthereau *et al*., 2014; Bosch *et al*., 2016; Labaume *et al*., 2016), while the exhumation of the Agly massif ceases (Gunnell *et al*., 2009; Ternois *et al*., 2019). The NPZ is finally tilted and uplifted by the exhumation of the Axial Zone related to crustal stacking. Consequently, the Boucheville and Bas-Agly synclines are now separated by the Agly Massif (Fig. 9d). Only small remnants of sedimentary cover are observed on the top of Agly massif. In this configuration, the North Pyrenean Fault corresponds to an inherited structure related to the rifting event and was only reactivated as a reverse fault during the end of collision. The main part of the deformation was accommodated by thick-skinned deformation expressed by the stacking of basement nappes, corresponding to the present-day Axial Zone. Thin-skinned deformation of the sedimentary cover was accommodated by the Upper Triassic decoupling layer. Consequently, the distribution of the deformation is drastically different between the basement and the sedimentary cover when an efficient decoupling layer

592 is present (e.g. Jammes et al., 2010; Jourdon et al., 2020). The presence of the Triassic evaporite
593 layer thus has considerably impacted the tectonic history of the eastern Pyrenees. First during
594 the rifting stage and then during the Pyrenean shortening.

595 After the main collision, the eastern Pyrenees was affected by normal faults associated with the
596 opening of Valencia Trough since the middle Oligocene (e.g. Roca *et al*., 1999; Roca, 2001;
597 Etheve *et al*., 2018; Jolivet et al., 2020).

598 5.4 Rift inheritances control the finite orogenic architecture

599 Classical models describing the geodynamic evolution of the Pyrenean range do not address the
600 early convergence and the onset of the collision of the two hyper-extended margins. Before the
601 two last decades, the Pyrenean rift was described as a narrow rift and hyperextension and mantle
602 exhumation were thus not considered in geodynamic models (e.g Choukroune et al., 1990;
603 Munoz, 1992; Beaumont et al., 2000; Canérot, 2016). Some recent models suggested that the
604 distal part of the rift system, corresponding to deep basins sitting on the exhumed mantle,
605 formed an accretionary prism during the subsequent early inversion (e.g. Mouthereau et al.,
606 2014; Ford et al., 2016). The early convergence setting is characterized by thin-skinned
607 tectonics in the sedimentary pile which corresponded to the former hyperextended domain
608 (mantle exhumation) (Fig. 9). A decollement propagates at the interface between Mesozoic
609 sediments and the basement (Paleozoic rocks and subcontinental mantle) within the Upper
610 Triassic evaporites. We further suggest that most of the distal rifted basin is transported over
611 the former necking domain along the former Cretaceous south-dipping detachment (Fig. 9).
612 This tectonic process is in agreement with recent studies promoting large displacements of
613 rifted basins along inherited decoupling layer (Gomez-Romeu et al., 2019; Labaume & Teixell,
614 2020). Rift-related inheritances (crustal structures and rheology) may fundamentally control the
615 development and the finite structure of orogens by controlling the depth of the decoupling layer
616 and its propagation (e.g., Tugend et al., 2014; Lacombe & Bellahsen, 2016; Gomez-Romeu et

al., 2019; Tavani et al., 2020; Lescoutre & Manatschal, 2020). Inversion of the hyperextended domains depends of the depth of the efficient decoupling layer. The positioning of the decoupling layer is variable and can be located at the interface between the basement and the sedimentary units (e.g. Bellahsen et al., 2012; Muñoz et al., 2013; this study) or in the serpentinized exhumed mantle which corresponds to the weakest part of rifted margins (Pérez-Gussinyé et al., 2001; Péron-Pinvidic et al., 2008), where deformation may preferentially initiate during the contractional deformation (Péron-Pinvidic et al., 2008; Lundin and Doré, 2011; Tugend et al., 2014 and 2015a; Gomez-Romeu et al., 2019). In the necking and proximal domains, the continental crust is thicker, and the decoupling layer consequently develops in the middle-lower crust (e.g.Pfiffner, 2017; Jourdon et al., 2019; Tavani et al., 2020). Therefore, during contractional deformation thick-skinned tectonics is prevailing, and inherited rift-related crustal structures may be reactivated (e.g. Froitzheim et al., 1988; Letouzey, 1990; Mitra et Mount, 1998; Brown et al., 1999; Domènech et al., 2016) or intersected by syn-tectonic structures (e.g. Bellahsen et al., 2012 ; Bellanger et al., 2014; Branellec et al., 2016). The tectonic history of the eastern Pyrenees as discussed in this paper thus shows the succession of two periods of the contractional deformation that led to the full inversion of the rifted margins. Other sections, further west, except for the Basque-Cantabrian basin with the Nappe des Marbres (Ducoux et al. 2019; Lescoutre and Manatschal, 2020), show a narrower IMZ where most units are pinched and vertical, thus obliterating the details of the shortening history. The Agly section and the Nappe des Marbres sections are thus key to unravel the early stages of the Pyrenean shortening with two stages, a first thin-skinned episode with decollement of the basin above the Triassic evaporites and a second thick-skinned episode leading to the present-day structure.

Conclusions

641 The eastern North Pyrenean Zone is thus an ideal locality to study the tectonic inversion and
642 integration of hyperextended rifted system (Internal Metamorphic Zone), associated with a pre-
643 rift decoupling layer, in an orogenic belt. By applying structural data and measured maximum
644 temperatures (T_{max}) estimated with the Raman Spectroscopy of Carbonaceous Materials
645 (RSCM) method, we show that a pre-kinematic decoupling layer has strongly impacted the
646 architecture of the Pyrenean belt, as well as the disposition of its sedimentary basins.

647 Concerning the thermal pattern, the Agly massif corresponded to a basement block separating
648 two metamorphic areas, the Boucheville syncline to the south and the Bas-Agly syncline to the
649 north. The Bas-Agly and Boucheville synclines are both affected by the Cretaceous H*T*/L*P*
650 metamorphism with T_{max} exceeding 550°C. Remnants of Mesozoic sediments observed on top
651 of the Agly massif is also affected by the H*T*/L*P* Pyrenean metamorphism with temperature
652 higher than 400°C but lower than in the Bas Agly syncline. A strong thermal contrast exists
653 between the Bas-Agly/Boucheville synclines and the St-Paul-de-Fenouillet syncline located to
654 the north. A thermal gap is also observed between Bas-Agly/Boucheville synclines and the
655 northeastern part of the Agly massif.

656 Structural observations confirm the T_{max} distribution measured in the Agly massif and Bas-Agly
657 syncline. The northeast part of the Agly massif composed by Silurian to Devonian shales
658 exposed various brittle and brittle-ductile shears without no pervasive ductile deformation,
659 while the Mesozoic sediments of the Bas-Agly syncline show an intense ductile deformation
660 with metric-scale boudinage and recumbent metric folds.

661 To explain thermal and structural gaps and the similarities between the Boucheville and Bas-
662 Agly synclines, we propose that the Bas-Agly syncline may correspond to an allochthonous
663 unit thrusted northward on top of the Agly massif and the St-Paul-de-Fenouillet syncline during
664 early stages of horizontal shortening (thin-skinned tectonics). The pre-orogenic Upper Triassic

evaporites decoupling layer and the low-angle normal faults inherited from the early Cretaceous rifting allowed the transport of the Mesozoic cover above a north-verging thrust and the substitution of the normal cover of the Agly massif by the metamorphic Bas-Agly syncline. Consequently, the Boucheville and Bas-Agly basins were initially parts of a single basin during the hyperextension rifting phase.

Acknowledgments

All the data used in this paper can be obtained in the figures, references, and supporting information. Additionally, these data are deposed in repository (PANGEA) at https://doi.pangaea.de/10.1594/PANGAEA.930199. The authors thank Stefano Tavani and an anonymous reviewer for thorough, thought-provoking reviews that substantially improved their initial submission. The authors also wish to thank Tectonics Editor Taylor Schildgen and Associate Editor Federico Rossetti for their comments and editorial support. This work has received funding from the Labex Voltaire and from the Institut Universitaire de France. It is a contribution of the Labex VOLTAIRE. This work was realized within the scope of the "Référentiel Géologique de la France" (RGF) funded by the French geological survey (BRGM). The authors are grateful to S. Janiec and J.G. Badin (ISTO) for the preparation of thin sections, A. Lahfid for precious helpful and advice for the Raman spectrometry. Many thanks to Charles Gumiaux, Jean-Claude Ringenbach, Etienne Legeay, Julie Tugend, Geoffroy Mohn and William Vetel for their help and fruitful discussions on the field.

References

Angrand, P., Ford, M., & Watts, A. B. (2018). Lateral variations in foreland flexure of a rifted continental margin: The Aquitaine Basin (SW France). Tectonics, 37(2), 430-449.

Azambre, B., Rossy, M., 1976. Le magmatisme alcalin d'age cretace, dans les Pyrenees occidentales et l'Arc basque; ses relations avec le metamorphisme et la tectonique. Bull. Soc. Geol. Fr. S7–XVIII, 1725–1728. doi:10.2113/gssgfbull.S7-XVIII.6.1725

Barnolas, A., Chiron, J. C., & Guérangé, B. (Eds.) (1996). Synthèse géologique et géophysique des Pyrénées: géophysique: cycle hercynien. Orléans, France: BRGM.

692 Beaumont, C., J. A. Muñoz, J. Hamilton, and P. Fullsack (2000), Factors controlling the Alpine
693 evolution of the central Pyrenees inferred from a comparison of observations and
694 geodynamical models, J. Geophys. Res., 105(B4), 8121–8145,
695 doi:10.1029/1999JB900390.

696 Bellahsen, N., Jolivet, L., Lacombe, O., Bellanger, M., Boutoux, A., Garcia, S., Mouthereau,
697 F., Le Pourhiet, L., Gumiaux, C., 2012. Mechanisms of margin inversion in the external
698 Western Alps; implications for crustal rheology. Tectonophysics 560–561, 62–83.
699 doi:10.1016/j.tecto.2012.06.022

700 Bellanger, M., Bellahsen, N., Jolivet, L., Baudin, T., Augier, R., Boutoux, A., 2014. Basement
701 shear zones development and shortening kinematics in the Ecrins Massif, Western Alps.
702 Tectonics 33, 84–111. doi:10.1002/2013TC003294

703 Berger, G.M., Bessière, G., Bilotte, M., Viallard, P., 1997. Carte géologique de la France (1/50
704 000), feuille Tuchan (1078), Bureau de recherches géologiques et minières, Orléans.

705 Berger, G.M., Fonteilles, M., Leblanc, D., Clauzon, G., Marchal, J.-P., Vautrelle C., 1993.
706 Notice explicative de la carte géologique de la France au 1/50.000, feuille de Rivesaltes
707 (1090), 119 pp., BRGM, Orléans.

708 Bernus-Maury, C., 1984. Etude des paragenèses caractéristiques du métamorphisme
709 mésozoïque dans la partie orientale des Pyrénées (French). Paris 6.

710 Bessière, G., Bilotte, M., Crochet, B., Peybernès, B., Tambareau, Y., Villate, J., 1989. Notice
711 explicative de la carte géologique de la France au 1/50.000, feuille de Quillan (1077),
712 98 pp., BRGM, Orléans.

713 Beyssac, O., Goffé, B., Chopin, C., Rouzaud, J.N., 2002. Raman spectra of carbonaceous
714 material in metasediments: a new geothermometer. J. Metamorph. Geol. 20, 859–871.
715 doi:10.1046/j.1525-1314.2002.00408.x

716 Beyssac, O., Rouzaud, J.-N., Goffé, B., Brunet, F., Chopin, C., 2002. Graphitization in a high-
717 pressure, low-temperature metamorphic gradient: a Raman microspectroscopy and
718 HRTEM study. Contrib. Mineral. Petrol. 143, 19.

719 Bles, J.L., Berger, G.M., 1982. Carte géologique de la France (1/50 000), feuille Leucate
720 (1079), Bureau de recherches géologiques et minières, Orléans.

721 Bosch, G., Teixell, A., Jolivet, M., Labaume, P., Stockli, D., Domènech, M., & Monié, P.
722 (2016). Timing of Eocene–Miocene thrust activity in the Western Axial Zone and
723 Chaînons Béarnais (west-Central Pyrenees) revealed by multi-method
724 thermochronology. Comptes Rendus Geoscience, 348(3–4), 246–256.
725 https://doi.org/10.1016/j.crte.2016.01.001

726 Bouhallier, H., Choukroune, P., Ballevre, M., 1991. Evolution structurale de la croûte profonde
727 hercynienne : exemple du massif de l'Agly (pyrenees orientales, france). Comptes
728 Rendus Académie Sci. Sér. 2 Mécanique Phys. Chim. Sci. Univers Sci. Terre 312, 647–
729 654.

730 Branellec, M., Niviere, B., Callot, J. P., & Ringenbach, J. C. (2016). Mechanisms of basin
731 contraction and reactivation in the basement-involved Malargüe fold-and-thrust belt,
732 Central Andes (34–36 S). Geological Magazine, 153(5-6), 926-944.

733 Brown, D., Alvarez-Marron, J., Perez-Estaun, A., Puchkov, V., Ayala, C., 1999. Basement
734 influence on foreland thrust and fold belt development; an example from the Southern
735 Urals. Tectonophysics 308, 459–472.

Canérot, J., 2016. The Iberian Plate: myth or reality? Bol. Geológico Min. 127, 563–574.

Canérot, J., 2008. Les Pyrénées: histoire géologique et itinéraires de découvertes, Atlantica-BRGM éditions. ed.

Canérot, J., 1988. Manifestations de l'halocinèse dans les chaînons béarnais (zone Nord-Pyrénéenne) au Crétacé inférieur. Comptes Rendus Académie Sci. Sér. 2 Mécanique Phys. Chim. Sci. Univers Sci. Terre 306, 1099–1102.

Canérot, J., Lenoble, J.L., 1993. Diapirisme cretace sur la marge iberique des Pyrenees occidentales; exemple du pic de Lauriolle; comparaisons avec l'Aquitaine, les Pyrenees centrales et orientales. Bull. Société Géologique Fr. 164, 719–726.

Casas, J. M., & Palacios, T. (2012). First biostratigraphical constraints on the pre-Upper Ordovician sequences of the Pyrenees based on organic-walled microfossils. Comptes Rendus Geoscience, 344(1), 50-56.

Chelalou, R., 2015. Formation et évolution du bassin de Boucheville, implication sur l'évolution tectonique, métamorphique et sédimentaire des bassins sédimentaires mésozoïques du Nord-Est des Pyrénées (phdthesis). Université Rennes 1.

Chelalou, R., Nalpas, T., Bousquet, R., Prevost, M., Lahfid, A., Poujol, M., Ringenbach, J.-C., Ballard, J.-F., 2016. New sedimentological, structural and paleo-thermicity data in the Boucheville Basin (eastern North Pyrenean Zone, France). Comptes Rendus - Géoscience 348, 312–321. doi:10.1016/j.crte.2015.11.008

Chevrot, S., Sylvander, M., Diaz, J., Martin, R., Mouthereau, F., Manatschal, G., ... & Ruiz, M. (2018). The non-cylindrical crustal architecture of the Pyrenees. Scientific reports, 8(1), 1-8.

Choukroune, P., 1976. Structure et évolution tectonique de la zone nord-pyrénéenne: analyse de la déformation dans une portion de chaîne à schistosité sub-verticale. Société géologique de France, Paris.

Choukroune, P., 1970. Contribution a l'etude structurale de la zone metamorphique nord-pyreneenne; tectonique et metamorphisme des formations secondaires de la foret de Boucheville (P.-O.); feuille au 1/50 000 Saint-Paul-de-Fenouillet. Struct. Metamorp 4, 49–63.

Choukroune, P., ECORS Team, 1989. The ECORS Pyrenean deep seismic profile reflection data and the overall structure of an orogenic belt. Tectonics 8, 23–39.

Choukroune, P., Pinet, B., Roure, F., Cazes, M., 1990a. Major Hercynian thrusts along the ECORS Pyrenees and Biscay lines. Bull. Soc. Geol. Fr. 6, 313–320.

Choukroune, P., Mattauer, M., 1978. Tectonique des plaques et Pyrenees: sur le fonctionnement de la faille transformante nord-pyreneenne; comparaisons avec des modeles actuels. Plate Tecton. Pyrenees Action North. Pyrenean Transform Fault Comp. 20, 689–700.

Clerc, C., Boulvais, P., Lagabrielle, Y., de St Blanquat, M., 2013. Ophicalcites from the northern Pyrenean belt: a field, petrographic and stable isotope study. Int. J. Earth Sci. 103, 141–163. doi:10.1007/s00531-013-0927-z

Clerc, C., Lagabrielle, Y., 2014. Thermal control on the modes of crustal thinning leading to mantle exhumation: Insights from the Cretaceous Pyrenean hot paleomargins. Tectonics 33, 2013TC003471. doi:10.1002/2013TC003471

Clerc, C., Lagabrielle, Y., Labaume, P., Ringenbach, J.-C., Vauchez, A., Nalpas, T., Bousquet, R., Ballard, J.-F., Lahfid, A., Fourcade, S., 2016. Basement – Cover decoupling and

progressive exhumation of metamorphic sediments at hot rifted margin. Insights from the Northeastern Pyrenean analog. Tectonophysics 686, 82–97. doi:10.1016/j.tecto.2016.07.022

Clerc, C., Lagabrielle, Y., Neumaier, M., Reynaud, J.-Y., de Saint Blanquat, M., 2012. Exhumation of subcontinental mantle rocks: evidence from ultramafic-bearing clastic deposits nearby the Lherz peridotite body, French Pyrenees. Bull. Soc. Geol. Fr. 183, 443–459.

Clerc, C., Lahfid, A., Monie, P., Lagabrielle, Y., Chopin, C., Poujol, M., Boulvais, P., Ringenbach, J.-C., Masini, E., de St Blanquat, M., 2015. High-temperature metamorphism during extreme thinning of the continental crust: a reappraisal of the North Pyrenean passive paleomargin. Solid Earth 6, 643–668. doi:10.5194/se-6-643-2015

Costa, S., Maluski, H., 1988. Use of the 40Ar- 39Ar stepwise heating method for dating mylonite zones: An example from the St. Barthe´le´my massif (Northern Pyrenees, France). Chem. Geol. Isot. Geosci. Sect. 72, 127–144. doi:10.1016/0168-9622(88)90061-9

Coleman, A. J., Duffy, O. B., & Jackson, C. A. L., 2019, Growth folds above propagating normal faults. Earth-Science Reviews, 102885.

Crittenden, M.D., Coney, P.J., Davis, G.H., 1980. Cordilleran metamorphic core complexes. Geol. Soc. Am. 490.

Crochet, B., Villate, J., Tambareau, Y., Bilotte, M., Bousquet, J.-P., Kuhfuss, A., Bouillin, J.-P., Gélard, J.-P., Bessière, G., Paris, J.-P., 1989. Carte géologique de la France (1/50 000), feuille Quillan (1077), Bureau de recherches géologiques et minières, Orléans.

Dauteuil, O., Ricou, L.E., 1989. Une circulation de fluides de haute-temperature a l'origine du metamorphisme cretace nord-pyreneen. Circ. High-Temp. Fluids Orig. North Pyrenean Cretac. Metamorph. 3, 237–250.

Davis, G.A., Lister, G.S., 1988. Detachment faulting in continental extension; Perspectives from the Southwestern U.S. Cordillera. Geol. Soc. Am. Spec. Pap. 218, 133–160. doi:10.1130/SPE218-p133

De Saint Blanquat, M., Lardeaux, J.M., Brunel, M., 1990. Petrological arguments for high-temperature extensional deformation in the Pyrenean Variscan crust (Saint Barthélémy massif, Ariège, France). Tectonophysics 177, 245–262. doi:10.1016/0040-1951(90)90284-F

Debroas, E.J., 1990. Le flysch noir albo-cenomanien temoin de la structuration albienne a senonienne de la Zone nord-pyreneenne en Bigorre (Hautes-Pyrenees, France). Bull. Société Géologique Fr. 6, 273–285.

Debroas, E.J., 1987. Le flysch a fucoides d'Uchentein temoin d'un escarpement turono-senonien inferieur de la paleofaille nord-pyreneenne, Pyrenees centrales, France. Fucoidal Flysch Uchentein Indic. Turonian-Low. Senonian Escarpm. Of 3, 77–93.

Delay, F. (1990). Etude structurale du massif de l'Agly (Pyrénées orientales). Mémoires de la Société Géologique du Nord, 17.

Delay, F., & Paquet, J. (1989). Tectonique ductile en extension dans le massif hercynien de l'Agly (zone nord-pyrénéenne): Comptes Rendus de l'Académie des Sciences) (Vol. 308, pp. 1637–1643).

824 Desegaulx, P., & Brunet, M. F. (1990). Tectonic subsidence of the Aquitaine basin since
825 Cretaceous times. Bulletin de la Société géologique de France, 8, 295-306.

826 Domènech, M., Teixell, A., Stockli, D.F., 2016. Magnitude of rift-related burial and orogenic
827 contraction in the Marrakech High Atlas revealed by zircon (U-Th)/He
828 thermochronology and thermal modeling. Tectonics 35, 2016TC004283.
829 doi:10.1002/2016TC004283

830 Ducoux, M. (2017). Structure, thermicité et évolution géodynamique de la Zone Interne
831 Métamorphique des Pyrénées (Doctoral dissertation).

832 Ducoux, Maxime; Jolivet, Laurent (2021): Peak metamorphic temperatures (Tmax) from the
833 eastern Pyrenees. PANGAEA, https://doi.pangaea.de/10.1594/PANGAEA.930199
834 (DOI registration in progress)

835 Ducoux, M., Jolivet, L., Callot, J-P., Aubourg, C., Masini, E., Lahfid, A., Homonnay, E.,
836 Cagnard, F., Gumiaux, C., & Baudin, T., 2019. The Nappe des Marbres unit of the
837 Basque-Cantabrian Basin: the tectono-thermal evolution of a fossil hyperextended rift
838 basin. Tectonics, …

839 Durand-Delga, M., 1964. Remarques sur la stratigraphie et la structure du Mésozoïque situé
840 entre Estagel et Perpignan (Pyrénées-Orientales). C. R. Acad. Sci. Paris 259, 837–840.

841 Duretz, T., Asti, R., Lagabrielle, Y., Brun, J. P., Jourdon, A., Clerc, C., & Corre, B. (2019).
842 Numerical modelling of Cretaceous Pyrenean Rifting: The interaction between mantle
843 exhumation and syn‐rift salt tectonics. Basin Research.

844 Etheve, N., Mohn, G., Frizon de Lamotte, D., Roca, E., Tugend, J., & Gómez-Romeu, J., 2018.
845 Extreme Mesozoic Crustal Thinning in the Eastern Iberia Margin: The Example of the
846 Columbrets Basin (Valencia Trough). Tectonics, 37(2), 636-662.

847 Ferrer, O., Roca, E., Jackson, M.P.A., Muñoz, J.A., 2009. Effects of Pyrenean contraction on
848 salt structures of the offshore Parentis Basin (Bay of Biscay). Trab. Geol. 29.
849 doi:10.17811/tdg.29.2009.%p

850 Fitzgerald, P.G., Muñoz, J.A., Coney, P.J., Baldwin, S.L., 1999. Asymmetric exhumation
851 across the Pyrenean orogen: implications for the tectonic evolution of a collisional
852 orogen. Earth Planet. Sci. Lett. 173, 157–170. doi:10.1016/S0012-821X(99)00225-3

853 Fonteilles, M. (1970). Géologie des terrains métamorphiques et granitiques du massif hercynien
854 de l'Agly (Pyrénées orientales). Bulletin de la Bureau de Récherches Géologiques et
855 Minéralogiques, 2, 21-72.

856 Fonteilles, M., Leblanc, D., Clauzon, G., Vaudin, J.-L., Berger, G.M., 1993. Carte géologique
857 de la France (1/50 000), feuille Rivesaltes (1090), Bureau de recherches géologiques et
858 minières, Orléans.

859 Froitzheim, N., Stets, J., Wurster, P., 1988. Aspects of Western High Atlas tectonics, in: In:
860 Jacobshagen, V. (Ed.), The Atlas System of Morocco, Lecture Notes in Earth Sciences.
861 Springer, Berlin, Heidelberg, pp. 219–244. doi:10.1007/BFb0011595

862 Garrido-Megias, A., Rios Aragues, L.M. (super a), 1972. Sintesis geologica del Secundario y
863 Terciario entre los rios Cinca y Segre (Pirineo Central de la vertiente sur pirenaica,
864 provincias de Huesca y Lerida). Summ. Mesoz. Tert. Geol. Cinca Segre Rivers Souther
865 83, 1–47.

Golberg, J.M., 1987. Le metamorphisme mesozoique dans la partie orientale des Pyrenees; relations avec l'evolution de la chaine au cretace. Universite des Sciences et Techniques du Languedoc, Centre Geologique et Geophysique : Montpellier, France, France.

Golberg, J.M., Leyreloup, A.F., 1990. High temperature-low pressure Cretaceous metamorphism related to crustal thinning (Eastern North Pyrenean Zone, France). Contrib. Mineral. Petrol. 104, 194–207. doi:10.1007/BF00306443

Gómez-Romeu, J., Masini, E., Tugend, J., Ducoux, M., & Kusznir, N. (2019). Role of rift structural inheritance in orogeny highlighted by the Western Pyrenees case-study. Tectonophysics.

Gorini, C., Le Marrec, A., Mauffret, A., 1993. Contribution to the structural and sedimentary history of the Gulf of Lions (western Mediterranean), from the ECORS profiles, industrial seismic pro-files and weIl data. Bull. Geol. Soc. France 164,353–363.

Gorini, C., Mauffret, A., Guennoc, P., Le Marrec, A., 1994. Structure of the Gulf of Lions (Northwestern Mediterranean Sea): a review. In: Mascle, A. (Ed.), Hydrocarbon and Petroleum Geology of France. Springer-Verlag, pp. 223–243.

Grool, A. R., Ford, M., Vergés, J., Huismans, R. S., Christophoul, F., & Dielforder, A. (2018). Insights into the crustal-scale dynamics of a doubly vergent orogen from a quantitative analysis of its forelands: A case study of the eastern Pyrenees. Tectonics, 37, 450–476. https://doi.org/10.1002/2017TC004731

Guille, B. T., Olivier, P., Paquette, J. L., Bosse, V., & Guillaume, D. (2019). Evolution of the middle crust of the Pyrenees during the Paleozoic: new data on the plutonic rocks from the North Pyrenean Agly massif. International Journal of Earth Sciences, 108(1), 245-265.

Gunnell, Y., Calvet, M., Brichau, S., Carter, A., Aguilar, J.-P., Zeyen, H., 2009. Low long-term erosion rates in high-energy mountain belts: Insights from thermo- and biochronology in the Eastern Pyrenees. Earth Planet. Sci. Lett. 278, 208–218. doi:10.1016/j.epsl.2008.12.004

Hogan, P. J., and K. D. W. Burbank (1996), Evolution of the Jaca piggy-back basin and emergence of the External Sierras, southern Pyrenees, in Tertiary Basins of Spain, edited by P. F. Friend and C. J. Dabrio, pp. 153–160, Cambridge Univ. Press, Cambridge, U. K.

Izquierdo‐Llavall, E., Menant, A., Aubourg, C., Callot, J. P., Hoareau, G., Camps, P., ... & Lahfid, A. Pre‐orogenic folds and syn‐orogenic basement tilts in an inverted hyperextended margin: the northern Pyrenees case study. Tectonics, e2019TC005719.

Jackson, M. P. A., & Vendeville, B. C. (1994). Regional extension as a geologic trigger for diapirism. Geological society of America bulletin, 106(1), 57-73.

James, V., Canerot, J., 1999. Diapirisme et structuration post-triasique des Pyrénées occidentale et de l'Aquitaine méridionale (France). Eclogae Geol. Helvetiae 63. doi:10.5169/seals-168647

Jammes, S., Manatschal, G., Lavier, L., 2010. Interaction between prerift salt and detachment faulting in hyperextended rift systems: The example of the Parentis and Mauléon basins (Bay of Biscay and western Pyrenees). AAPG Bull., 2010b 94, 957–975. doi:10.1306/12090909116

Jammes, S., Manatschal, G., Lavier, L., Masini, E., 2009. Tectonosedimentary evolution related to extreme crustal thinning ahead of a propagating ocean: Example of the western Pyrenees. Tectonics 28, TC4012. doi:10.1029/2008TC002406

Jolivet, L., Romagny, A., Gorini, C., Maillard, A., Thinon, I., Couëffé, R., Ducoux, M., Séranne, M., 2020. Fast dismantling of a mountain belt by mantle flow: late-orogenic evolution of Pyrenees and Liguro-Provençal rifting. Tectonophysics 776, 228312, doi.org/228310.221016/j.tecto.222019.228312.

Jolivet, M., Labaume, P., Monié, P., Brunel, M., Arnaud, N., Campani, M., 2007. Thermochronology constraints for the propagation sequence of the south Pyrenean basement thrust system (France-Spain). Tectonics 26, TC5007. https://doi.org/10.1029/2006TC002080.

Jourdon, A., Le Pourhiet, L., Mouthereau, F., & Masini, E. (2019). Role of rift maturity on the architecture and shortening distribution in mountain belts. Earth and Planetary Science Letters, 512, 89-99.

Jourdon, A., Mouthereau, F., Le Pourhiet, L., & Callot, J. P. (2020). Topographic and tectonic evolution of mountain belts controlled by salt thickness and rift architecture. Tectonics, 39(1), e2019TC005903.

Labaume, P., Meresse, F., Jolivet, M., & Teixell, A. (2016). Exhumation sequence of the basement thrust units in the west-central Pyrenees. Constraints from apatite fission track analysis. Geogaceta, 60, 11–14.

Labaume, P., Teixell, A., 2020. Evolution of salt structures of the Pyrenean rift (Chaînons Béarnais, France): From hyper-extension to tectonic inversion. Tectonophysics, https://doi.org/10.1016/j.tecto.2020.228451.

Lacombe, O., and Bellahsen, N., 2016, Thick-skinned tectonics and basement-involved fold–thrust belts: insights from selected Cenozoic orogens: Geological Magazine, v. 153, p. 763–810, doi:10.1017/S0016756816000078.

Lagabrielle, Y., Bodinier, J.-L., 2008. Submarine reworking of exhumed subcontinental mantle rocks; field evidence from the Lherz peridotites, French Pyrenees. Terra Nova 20, 11–21. doi:10.1111/j.1365-3121.2007.00781.x

Lagabrielle, Y., Clerc, C., Vauchez, A., Lahfid, A., Labaume, P., Azambre, B., Fourcade, S., Dautria, J.-M., 2016. Very high geothermal gradient during mantle exhumation recorded in mylonitic marbles and carbonate breccias from a Mesozoic Pyrenean palaeomargin (Lherz area, North Pyrenean Zone, France). Comptes Rendus Geosci., From rifting to mountain building: the Pyrenean Belt 348, 290–300. doi:10.1016/j.crte.2015.11.004

Lagabrielle, Y., Labaume, P., de Saint Blanquat, M., 2010. Mantle exhumation, crustal denudation, and gravity tectonics during Cretaceous rifting in the Pyrenean realm (SW Europe): Insights from the geological setting of the lherzolite bodies. Tectonics 29, TC4012. doi:10.1029/2009TC002588

Lahfid, A., Beyssac, O., Deville, E., Negro, F., Chopin, C., Goffe, B., 2010. Evolution of the Raman spectrum of carbonaceous material in low-grade metasediments of the Glarus Alps (Switzerland). Terra Nova 22, 354–360. doi:10.1111/j.1365-3121.2010.00956.x

Légier, C., Tempier, C., Vauchez, A., 1987. Tectoniques tangentielle ductile synmétamorphe d'âge Crétacé supérieur dans la couverture du massif de l'Agly (zone Nord-pyrénéenne orientale). C. R. Acad. Sci. Paris 305, 907–911.

Lemoine, M., bas, T., Arnaud-Vanneau, A., Arnaud, H., Dumont, T., Gidon, M., Bourbon, M., de Graziansky, P.C., Rudkiewicz, J.L., Mégard-Galli, J., 1986. The continental margin of the mesozoic tethys in the western alps. Marine and petroleum geology 3, 179-199.

Lescoutre, R., & Manatschal, G. (2020). Role of rift-inheritance and segmentation for orogenic evolution: example from the Pyrenean-Cantabrian systemRôle de l'héritage associé au rift et à sa segmentation pour l'évolution orogénique: exemple du système pyrénéo-cantabrique. Bulletin de la Société Géologique de France, 191(1). https://doi.org/10.1051/bsgf/2020021

Letouzey, J., 1990. Fault reactivation, inversion and foldthrust belt, in Petroleum and tectonics in Mobile Belts, edited by J. Letouzey. Tech. Paris 101–128.

Lopez-Mir, B., Muñoz, J. A., & Senz, J. G. (2014). Restoration of basins driven by extension and salt tectonics: Example from the Cotiella Basin in the central Pyrenees. Journal of Structural Geology, 69, 147-162.

Lundin, E.R., Doré, A.G., 2011. Hyperextension, serpentinization, and weakening: a new paradigm for rifted margin compressional deformation. Geology 39, 347–350. https://doi.org/10.1130/G31499.1.

Manatschal, G., Lavier, L., & Chenin, P. (2015). The role of inheritance in structuring hyperextended rift systems: Some considerations based on observations and numerical modeling. Gondwana Research, 27(1), 140-164.

Martinez-Peña, M., and A. Casas-Sainz (2003), Cretaceous–Tertiary tectonic inversion of the Cotiella Basin (southern Pyrenees, Spain), Int. J. Earth Sci. (Geol. Rundsch.), 92(1), 99–113, doi:10.1007/s00531-002-0283-x.

Masini, E., Manatschal, G., Tugend, J., Mohn, G., Flament, J.-M., 2014. The tectono-sedimentary evolution of a hyper-extended rift basin; the example of the Arzacq-Mauleon rift system (western Pyrenees, SW France). Int. J. Earth Sci. Geol. Rundsch. 103, 1569–1596. doi:10.1007/s00531-014-1023-8

Mattauer, M., 1968. Les traits structuraux essentiels de la Chaîne des Pyrenées. Essent. Struct. Traits Pyrenees 10, 3–11.

Mauffret, A., Pascal, G., Maillard, A., Gorini, C., 1995. Tectonics and deep structure of the north-western Mediterranean basin. Mar. Pet. Geol. 12, 645–666.

Mauffret, A., Durand de Grossouvre, B., Dos Reis, A.T., Gorini, C., Nercessian, A., 2001. Structural geometry in the eastern Pyrenees and western Gulf of Lion (Western Mediterranean). J. Struct. Geol. 23, 1701–1726.

McClay, K., Munoz, J.-A., Garcia-Senz, J., 2004. Extensional salt tectonics in a contractional orogen; a newly identified tectonic event in the Spanish Pyrenees. Geol. Boulder 32, 737–740. doi:10.1130/G20565.1

Michard, A.V., Allègre, C.J., 1975. A study of the formation and history of a piece of continental crust by 87Rb-87Sr method: The case of the French oriental Pyrénées. Contrib. Mineral. Petrol. 50, 257–285. doi:10.1007/BF00394853

Millán Garrido, H. (2006), Estructura y cinemática del frente de cabalgamiento surpirenaico en las Sierras Exteriores aragonesas, in Colección de Estudios Altoaragoneses, vol. 53, Instituto de Estudios Altoaragoneses, Huesca, Spain.

Millán Garrido, H., E. L. Pueyo Morer, M. Aurell Cardona, A. Aguado Luzón, B. Oliva Urcia, M. B. Martínez Peña, and A. Pocoví (2000), Actividad tectonica registrada en los

depósitos terciarios del frente meridional del Pirineo central, Rev. Soc. Geol. Esp., 13, 279–300.

Mouthereau, F., Watts, A.B., Burov, E., 2013. Structure of orogenic belts controlled by lithosphere age. Nat. Geosci. 6, 785–789. doi:10.1038/ngeo1902

Mouthereau, F., Filleaudeau, P.-Y., Vacherat, A., Pik, R., Lacombe, O., Fellin, M.G., Castelltort, S., Christophoul, F., Masini, E., 2014. Placing limits to shortening evolution in the Pyrenees: Role of margin architecture and implications for the Iberia/Europe convergence. Tectonics 33, 2014TC003663. doi:10.1002/2014TC003663

Mitra, S., Mount, V.S., 1998. Foreland Basement-Involved Structures. AAPG Bull. 82, 70–109.

Muñoz, J.A., 1992. Evolution of a continental collision belt; ECORS-Pyrenees crustal balanced cross-section. In: MCCLAY, K. R. (ed) Thrust tectonics. Chapman & Hall : London, United Kingdom, pp. 235–246.

Muñoz, J.A., 2002. The Pyrenees. In: GIBBONS, W. & MORENO, M. T. (eds) The geology of Spain. Geological Society, London, p. 370–385.

Muñoz, J.A., Beamud, E., Fernández, O., Arbués, P., Dinarès-Turell, J., and Poblet, J., 2013, The Ainsa Fold and thrust oblique zone of the central Pyrenees: Kinematics of a curved contractional system from paleomagnetic and structural data: Tectonics, v. 32, p. 1–34, doi:10.1002/tect.20070.

Odlum, M. L., & Stockli, D. F. (2019). Thermotectonic evolution of the North Pyrenean Agly massif during Early Cretaceous hyperextension using multi-mineral U-Pb thermochronometry. Tectonics, 38, 1509–1531. https://doi.org/10.1029/2018TC005298

Oliva-Urcia, B., E. Beamud, M. Garcés, C. Arenas, R. Soto, E. L. Pueyo, and G. Pardo (2015), New magnetostratigraphic dating in the Palaeogene syntectonic sediments of the west-central Pyrenees: Tectonostratigraphic implications, in Palaeomagnetism in Fold and Thrust Belts: New Perpectives, edited by E. L. Pueyo, Geol. Soc. Spec. Publ., 425, doi:10.1144/SP425.5.

Olivier, P., Gleizes, G., Paquette, J.L., 2004. Gneiss domes and granite emplacement in an obliquely convergent regime: New interpretation of the Variscan Agly massif (Eastern Pyrenees, France). Geol. Soc. Am. Spec. Pap. 380, 229–242. doi:10.1130/0-8137-2380-9.229

Olivier, P., Gleizes, G., Paquette, J.-L., Sáez, C.M., 2008. Structure and U–Pb dating of the Saint-Arnac pluton and the Ansignan charnockite (Agly massif): a cross-section from the upper to the middle crust of the Variscan Eastern Pyrenees. J. Geol. Soc. 165, 141–152. doi:10.1144/0016-76492006-185

Olivier, P. (2013), Comment on “Preorogenic exhumation of the North Pyrenean Agly massif (Eastern Pyrenees-France)” by A. Vauchez *et al*., Tectonics, 32, 821–822, doi:10.1002/tect.20049

Ortiz, A., Guillocheau, F., Lasseur, E., Briais, J., Robin, C., Serrano, O., & Fillon, C., 2020, Sediment routing system and sink preservation during the post-orogenic evolution of a retro-foreland basin: The case example of the North Pyrenean (Aquitaine, Bay of Biscay) Basins. Marine and Petroleum Geology, 112, 104085.

Paquet, J., Mansy, J.-L., 1991. La structure de l’Est des Pyrénées (transversales du massif de l’Agly) : un exemple d’amincissement crustal. Comptes Rendus Académie Sci. Sér. 2 Mécanique Phys. Chim. Sci. Univers Sci. Terre 312, 913–919.

Passchier, C.W., 1984. Mylonite-dominated footwall geometry in a shear zone, central Pyrenees. Geol. Mag. 121, 429–436. doi:10.1017/S0016756800029964

Pasteris, J., Wopenka, B., 1991. Raman-Spectra of Graphite as Indicators of Degree of Metamorphism. Can. Mineral. 29, 1–9.

Pasteris, J.D., 1989. In situ analysis in geological thin-sections by laser Raman microprobe spectroscopy; a cautionary note. Appl. Spectrosc. 567–570.

Pérez-Gussinyé, M., Reston, T.J., Phipps Morgan, J., 2001. Serpentinization and magmatism during extension at non-volcanic margins: the effect of initial lithospheric structure. Geol. Soc. London, Spec. Publ. 187, 551–576. https://doi.org/10.1144/GSL.SP.2001.187.01.27.

Péron-Pinvidic, G., Manatschal, G., Dean, S.M., Minshull, T.A., 2008. Compressional structures on the West Iberia rifted margin: Controls on their distribution. In:Johnson, H. (Ed.), The Nature and Origin of Compression in Passive Margins. Geol.Soc. London, Spec. Publ. vol. 306. pp. 169–183. https://doi.org/10.1144/SP306.8.

Pfiffner, O.A., 2017, Thick-Skinned and Thin-Skinned Tectonics: A Global Perspective: Geosciences, v. 7, p. 71, doi:10.3390/geosciences7030071.

Poujol, M., Boulvais, P., Kosler, J., 2010. Regional-scale Cretaceous albitization in the Pyrenees: evidence from in situ U–Th–Pb dating of monazite, titanite and zircon. J. Geol. Soc. 167, 751–767. doi:10.1144/0016-76492009-144

Ravier, J., 1959. Le metamorphisme des terrains secondaires des Pyrenees. Memoires Soc. Geol. Fr. Nouv. Ser. 38.

Roca, E., 2001. The Northwest Mediterranean Basin (Valencia Trough, gulf of Lions and Liguro-Provençal basins): structure and geodynamic evolution, in Ziegler, P. A., Cavazza, W., Robertson, A. H. F., and Crasquin-Soleau, S., eds., Peri-Tethys Memoir 6: Pery-Tethyan Rift/Wrench Basins and Passive Margins. Mémoires Muséum National d'HistoireNaturelle, 186: Paris, 671–706.

Roca, E., Sans, M., Cabrera, L., Marzo, M., 1999. Oligocene to Middle Miocene evolution of the central Catalan margin (northwestern Mediterranean). Tectonophysics 315, 209–229. doi:10.1016/S0040-1951(99)00289-9

Roure, F., P. Choukroune, X. Beràstegui, J. A. Muñoz, A. Villien, P. Matheron, M. Bareyt, M. Séguret, P. Camara, and J. Déramond (1989), ECORS deep seismic data and balanced cross sections: Geometric constraints on the evolution of the Pyrenees, Tectonics, 8(1), 41–50, doi:10.1029/TC008i001p00041.

Rowan, M.G., 2014, Passive-margin salt basins; hyperextension, evaporite deposition, and salt tectonics. Basin Res. 26, 154–182. doi:10.1111/bre.12043

Rushlow, C.R., Barnes, J.B., Ehlers, T.A., Vergés, J., 2013. Exhumation of the southern Pyrenean fold-thrust belt (Spain) from orogenic growth to decay. Tectonics 32, 843-860. doi:10.1002/tect.20030

Saura, E., L. Ardèvol i Oró, A. Teixell, and J. Vergés (2016), Rising and falling diapirs, shifting depocenters, and flap overturning in the Cretaceous Sopeira and Sant Gervàs subbasins (Ribagorça Basin, southern Pyrenees), Tectonics, 35, 638–662, doi:10.1002/2015TC004001.

Scharf, A., Handy, M.R., Ziemann, M.A., Schmid, S.M., 2013. Peak-temperature patterns of polyphase metamorphism resulting from accretion, subduction and collision (eastern

Tauern Window, European Alps); a study with Raman microspectroscopy on carbonaceous material (RSCM). J. Metamorph. Geol. 31, 863–880. doi:10.1111/jmg.12048

Tavani, S., Camanni, G., Nappo, M., Snidero, M., Ascione, A., Valente, E., Gharabeigli, G., Morsalnejad, D., and Mazzoli, S., 2020, The Mountain Front Flexure in the Lurestan region of the Zagros belt: Crustal architecture and role of structural inheritances: Journal of Structural Geology, v. 135, p. 104022, doi:10.1016/j.jsg.2020.104022.

Ternet, Y., Colchen, M., Debroas, E.-J., Azambre, B., Debon, F., Bouchez, J.L., Gleizes, G., Leblanc, D., Bakalowicz, M., Jauzion, G., Mangin, A., Soulé, J.-C., 1997. Notice explicative de la carte géologique de la France au 1/50.000, feuille de Aulus-les-Bains (1086), 146 pp., BRGM, Orléans.

Ternois, S., Odlum, M., Ford, M., Pik, R., Stockli, D., Tibari, B., *et al*. (2019). Thermochronological evidence of early orogenesis, eastern Pyrenees, France. Tectonics, 38, 1308–1336. https://doi.org/10.1029/2018TC005254

Teixell, A. (1996), The Ansó transect of the southern Pyrenees: Basement and cover thrust geometries, J. Geol. Soc., 153, 301–310.

Teixell, A. (1998), Crustal structure and orogenic material budget in the west central Pyrenees, Tectonics, 17(3), 395–406, doi:10.1029/98TC00561.

Teixell, A., Labaume, P., & Lagabrielle, Y., 2016, The crustal evolution of the west-central Pyrenees revisited: inferences from a new kinematic scenario. Comptes Rendus Geoscience, 348(3-4), 257-267.

Tugend, J., Manatschal, G., Kusznir, N.J., Masini, E., Mohn, G., Thinon, I., 2014. Formation and deformation of hyperextended rift systems; insights from rift domain mapping in the Bay of Biscay-Pyrenees. Tectonics 33, 1239–1276. doi:10.1002/2014TC003529

Tugend, J., Manatschal, G., Kusznir, N.J., 2015. Spatial and temporal evolution of hyperextended rift systems: Implication for the nature, kinematics, and timing of the Iberian- European plate boundary. Geology 15–18. https://doi.org/10.1130/G36072.1.

Vacherat, A., Mouthereau, F., Pik, R., Bellahsen, N., Gautheron, C., Bernet, M., Daudet, M., Balansa, J., Tibari, B., Pinna Jamme, R., Radal, J., 2016. Rift-to-collision transition recorded by tectonothermal evolution of the northern Pyrenees. Tectonics 35, 907.

Vacherat, A., Mouthereau, F., Pik, R., Bernet, M., Gautheron, C., Masini, E., Le Pourhiet, L., Tibari, B., Lahfid, A., 2014. Thermal imprint of rift-related processes in orogens as recorded in the Pyrenees. Earth Planet. Sci. Lett. 408, 296–306. doi:10.1016/j.epsl.2014.10.014

Vanardois J, Trap P, Goncalves P, Marquer D, Gremmel J, Siron G, Baudin T. 2020. Kinematics, deformation partitioning and late Variscan magmatism in the Agly massif, Eastern Pyrenees, France, BSGF - Earth Sciences Bulletin 191: 15.

Vauchez, A., Clerc, C., Bestani, L., Lagabrielle, Y., Chauvet, A., Lahfid, A., Mainprice, D., 2013. Pre-orogenic exhumation of the north Pyrenean Agly massif (eastern Pyrenees, France). Tectonics 32, 95–106. doi:10.1002/tect.20015

Vergés, J., and García-Senz, J., 2001. Mesozoic evolution and Cainozoic inversion of the Pyrenean rift, in Peri-Tethyan Rift/Wrench Basins and Passive Margins, edited by P. A. Ziegler et al., mémoire, pp. 187– 212,

Verges, J., Fernandez, M., Martinez, A., 2002. The Pyrenean orogen; pre-, syn-, and post-collisional evolution. J. Virtual Explor. 8, 57–76.

Vielzeuf, D., and J. Kornprobst (1984), Crustal splitting and the emplacement of Pyrenean lherzolites and granulites, Earth Planet. Sci. Lett., 67(1), 87–96, doi:10.1016/0012-821X(84)90041-4.

Watts, A.B., Lamb, S.H., Fairhead, J.D., Dewey, J.F., 1995. Lithospheric flexure and bending of the Central Andes. Earth Planet. Sci. Lett. 134, 9–21. doi:10.1016/0012-821X(95)00095-T

Wehr, H., Chevrot, S., Courrioux, G., Guillen, A., 2018. A three-dimensional model of the Pyrenees and their foreland basins from geological and gravimetric data. Tectonophysics 734-735, 16-32; https://doi.org/10.1016/j.tecto.2018.1003.1017.

Whitchurch, A.L., Carter, A., Sinclair, H.D., Duller, R.A., Whittaker, A.C., Allen, P.A., 2011. Sediment routing system evolution within a diachronously uplifting orogen: Insights from detrital zircon thermochronological analyses from the South-Central Pyrenees. Am. J. Sci. 311, 442–482. doi:10.2475/05.2011.03

Wickham, S. M., & Oxburgh, E. R. (1986). A rifted tectonic setting for Hercynian high‐thermal gradient metamorphism in the Pyrenees. Tectonophysics, 129(1−4), 53−69. https://doi.org/10.1016/0040‐1951(86)90245‐3

Wopenka, B., Pasteris, J.D., 1993. Structural characterization of kerogens to granulite-facies graphite : applicability of Raman microprobe spectroscopy. Am. Mineral. 78, 533–557.

Yelland, A.J., 1991. Thermo-tectonics of the Pyrenees and Provence from fission track studies. Ph.D. thesis, University of London.

Figures captions

Figure 1: Simplified structural map of the Pyrenean belt. Only main “alpine” thrusts and faults are represented: North-Pyrenean Frontal Thrust (NPFT), South-Pyrenean Frontal Thrust (SPFT), and North-Pyrenean Fault. The Internal Metamorphic Zone (IMZ, orange in the figure) is located in the North Pyrenean Zone (NPZ) and crops out along the strike of the belt. The study area is located in the eastern part of this belt.

Figure 2: Geological map of the eastern part of the North Pyrenean Zone (localization on Fig. 1) (after Crochet *et al*., 1989; Berger *et al*., 1997; Bles and Berger, 1982; Fonteilles *et al*., 1993) with T_{max} measured with Raman spectrometry (Chelalou, 2015 (in blue); Clerc *et al*., 2015 (in black) and this study (in red)) and thermobarometry estimates (Golberg and Leyreloup, 1990). Localisation of Mesozoic sequences remnants on the Agly massif are pointed out by numbers:

(1) Serre de Cors; (2) Serre de Verges; (3) Roc de Lansac; (4) Lake Caramany and (5) Agly dam.

Figure 3: Isometamorphic map of the H*T*/L*P* metamorphism distribution in the eastern part of the North Pyrenean Zone.

Figure 4: Structural map of the eastern part of the North Pyrenean Zone (localization on Fig. 1) (after Crochet *et al*., 1989; Berger *et al*., 1997; Bles and Berger, 1982; Fonteilles *et al*., 1993). This map displays the different tectono-stratigraphic units and the detail of structural framework (trajectories of foliation and cleavage; lineations and folds). Early convergence-related fault are drawn in orange and late convergence-related fault in red.

Figure 5: field photographs and interpretations of the observed deformation in the Paleozoic sediments of the Agly massif. a) top-to-the N normal shears. b) top-to-the S reverse shears.

Figure 6: field photographs and interpretations of the observed deformation in Mesozoic Bas-Agly sedimentary cover. a) big picture on Rhaetian and Liassic sediments of the southern Bas-Agly, modified after Clerc *et al.* (2016). b) zoom on recumbent fold with top-to-the north verging. c) pure shear deformation and hectometer-scale boudinaged of Liassic sediments.

Figure 7: Geological cross sections through the eastern part of the IMZ illustrating the relationships between the Bas-Agly syncline and surroundings units. Legend is similar to Figure 2.

Figure 8: Comparison of thermal structure for two endmembers: (a) a detachment system forming a MCC and (b) a thrust system. Structures are sole in the middle-lower continental crust and isotherms represent static maximum temperatures reached by rocks.

Figure 9: Geodynamical model of the eastern part of the NPZ illustrating a structural evolution from the rifting event to the present, modified after Ternois *et al.* (2019). Four steps of

1186 restoration are depicted. SFPT: South Pyrenean Frontal Thrust; NPF: North Pyrenean Fault;
1187 LTFF: La-Tour-de-France Fault; TF: Tautavel Fault; NPFT: North Pyrenean Frontal Thrust.
1188 See text for explanations.

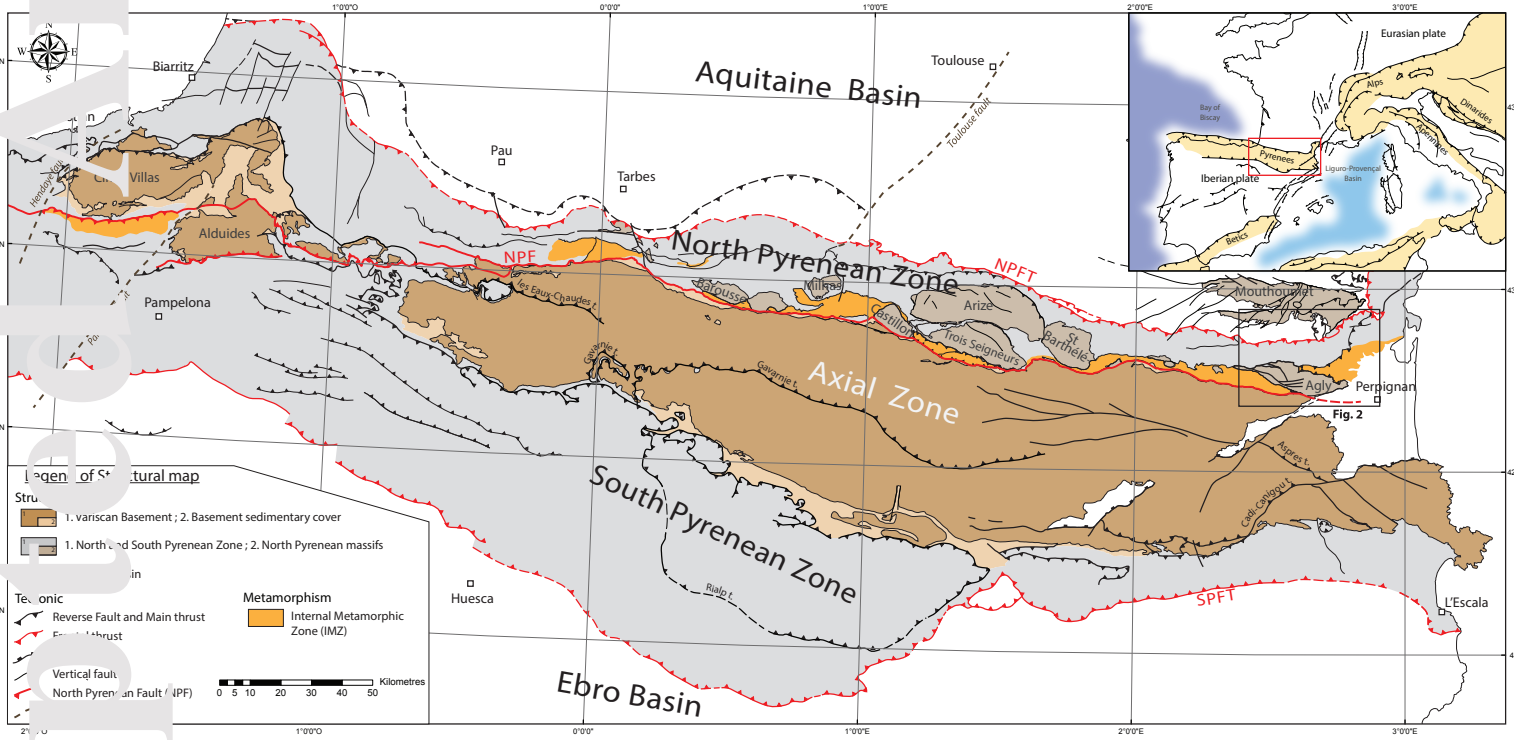

This article has been accepted for publication and undergone full peer review but has not been through the copyediting, typesetting, pagination and proofreading process, which may lead to differences between this version and the Version of Record. Please cite this article as doi: 10.1029/2020TC006512.

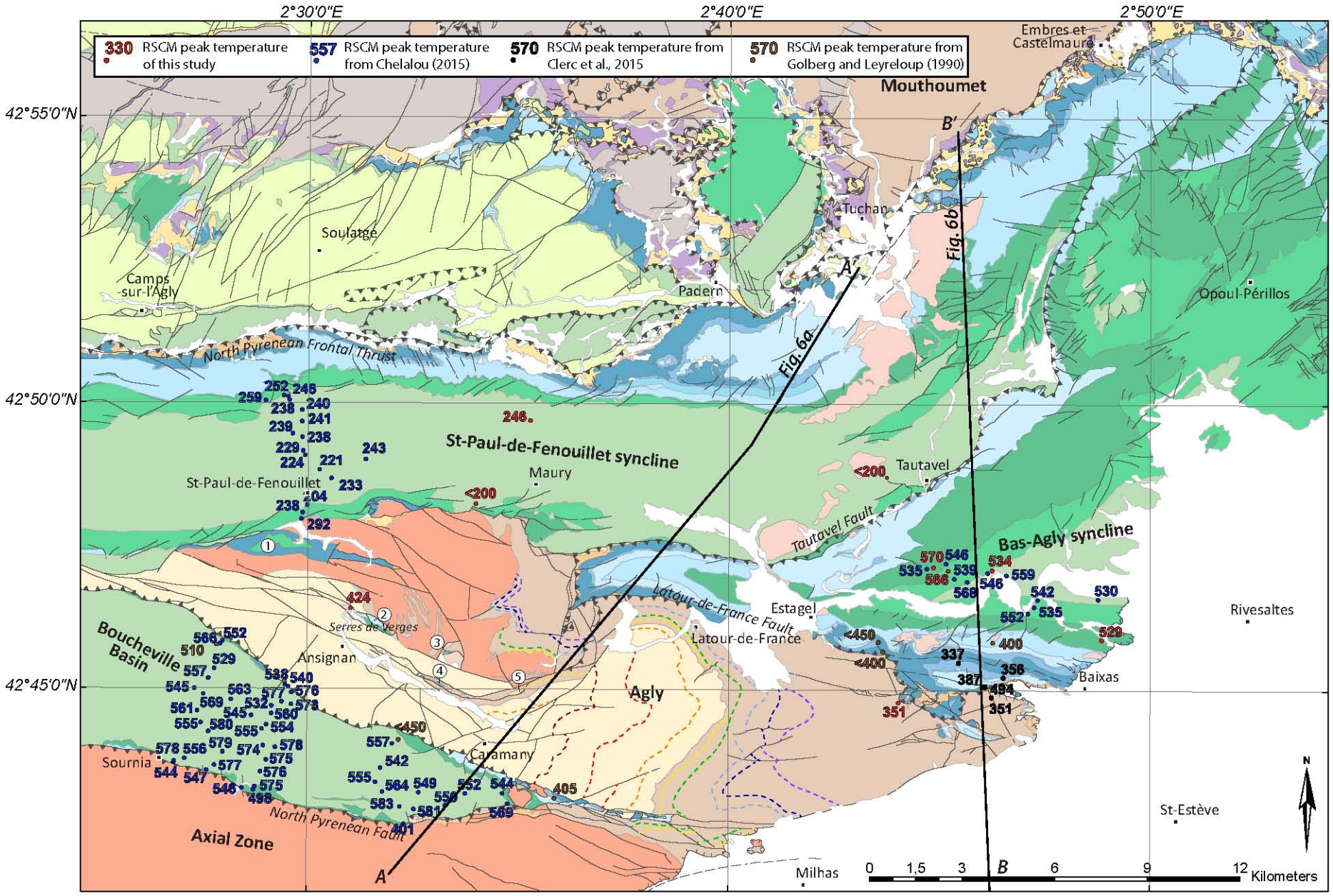
330 RSCM peak temperature of this study
557 RSCM peak temperature from Chelalou (2015)
570 RSCM peak temperature from Clerc et al., 2015
570 RSCM peak temperature from Golberg and Leyreloup (1990)
2°30'0"E
2°40'0"E
2°50'0"E
42°55'0"N
42°50'0"N
42°45'0"N
Embres et Castelmaure
Mouthoumet
Tuchan
Soulatgé
Camps-sur-l'Agly
Padern
Opoul-Périllos
North Pyrenean Frontal Thrust
St-Paul-de-Fenouillet syncline
St-Paul-de-Fenouillet
Maury
Tautavel
Tautavel Fault
Bas-Agly syncline
Latour-de-France Fault
Estagel
Latour-de-France
Rivesaltes
Serres de Verges
Ansignan
Boucheville Basin
Agly
Baixas
Sournia
Caramany
St-Estève
Milhas
North Pyrenean Fault
Axial Zone
Fig. 6a
Fig. 6b
A
A'
B
B'
0 1,5 3 6 9 12 Kilometers
N
Quaternary
Paleogen (clay)
Turonian to Maastrichtian (Sandstone, marls and limestone)
Albian to lower Cenomanian (Marls)
Aptian (Marls and limestones)
Berriasian to Baremian (Limestones)
Oxfordian to Tithonian (Limestones)
Bajocian to Callovian (Limestones and dolomites)
Bajocian to Tithonian (Limestones and dolomites)
Pliensbachian to Aalenian (marls and limestones)
Hettangian to Sinemurian (Limestones and dolomites)
Rhaetian (Clays, limestones, sandstones, dolomites and marls)
Upper Triassic (Marls, gypsum, sandstones and dolomites)
Middle to Lower Triassic (Conglomerates, sandstones, limestones, marls and dolomites)
③ Remnants of Mesozoic sequences
Carboniferous (Lydian stone, limestones, conglomerates)
Ordovician to Devonian (Micaschists, shales, sandstone and limestone)
Plutonic rocks (Granits)
Agly paragneisses and orthogneisses
Variscan Metamorphism
Metamorphic gradient
Zi
Zh
Zg
Zf
Ze
Zd
Zc
Zb
Za

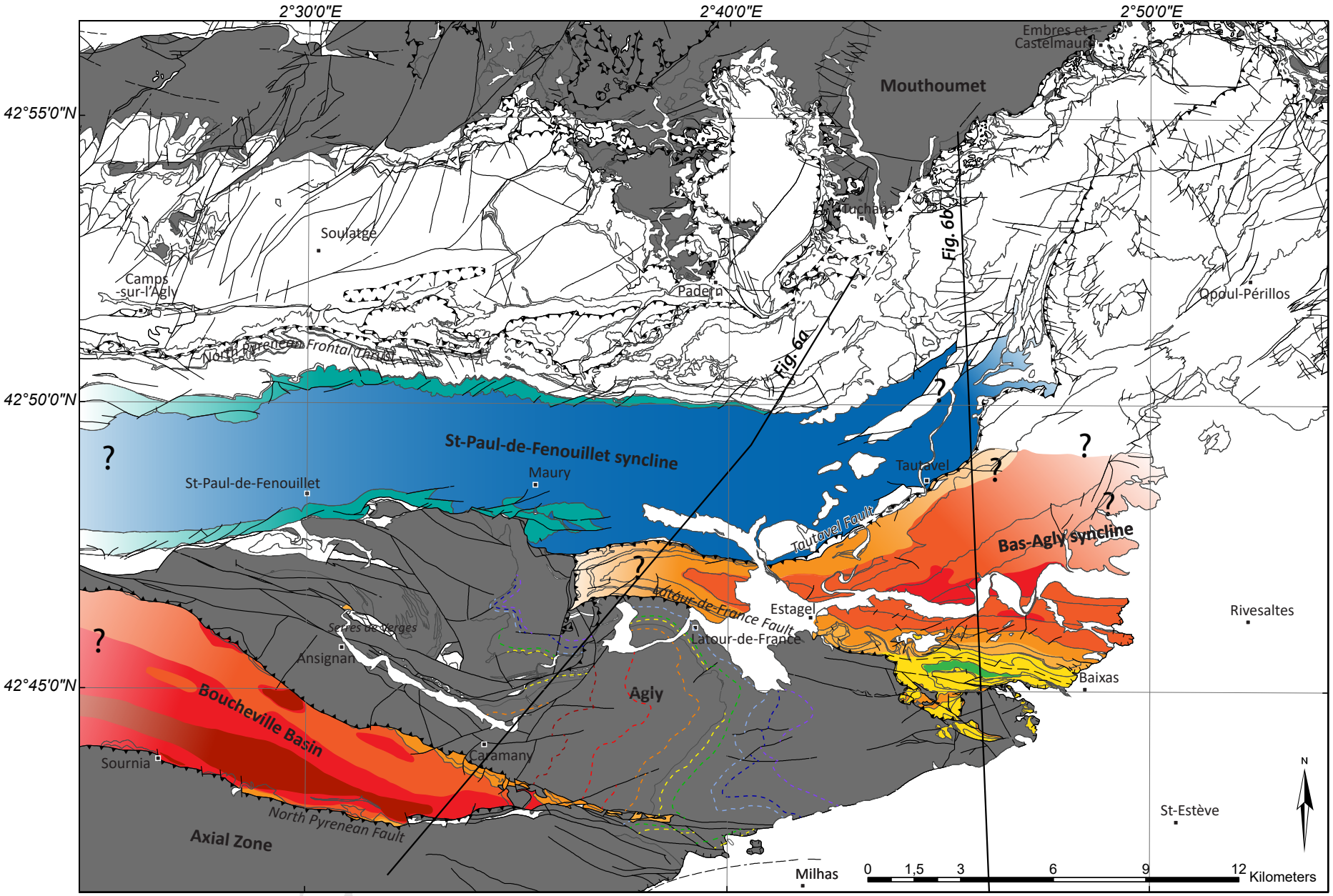

Legend of structural map

Tectono-stratigraphic Units

- *Post-rift*
  - Turonian to Maastrichtian
- *Syn-rift*
  - Albian to Cenomanian
  - Late Aptian
- *Pre-rift*
  - Rhaetian to Aptian
  - Upper Triassic and Ophite
  - Permian to middle Triassic
- *Basement*
  - Metasediments
  - Metamorphic rocks
  - Plutonic rocks

Details of structures

- *Pyrenean Structures*

Structural data

- (S_{0-1}) Direction trajectories of ductile foliation
- (S_2) Direction trajectories of cleavage
- Cleavage front
- Stretching lineations
- Mineral lineations
- ductile lineations (after *Clerc et al., 2015*)

Salt tectonic- related structures

- Diapiric zones and rafts

Faults

- Main early convergence faults
- Main late convergence faults
- Minor thrusts
- Undifferentiated faults
- Late breccias (décollement plane ?)

Folds

- Large scale Synform
- Large scale Antiform
- Local (dm to m) folds with plunge value of axis

- *Variscan Structures*
  - Thrusts and reverse fault
  - Extensional fault

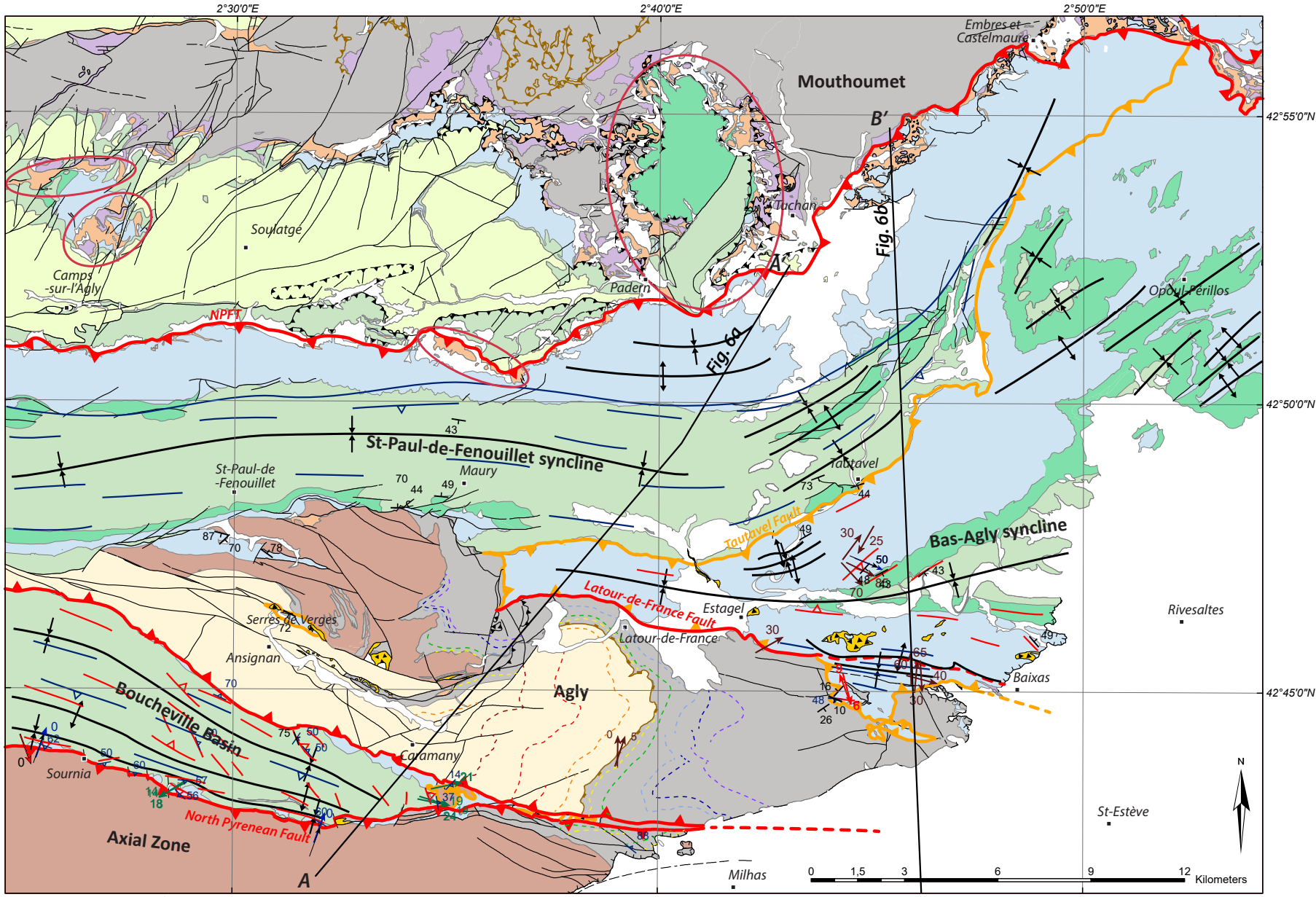


a

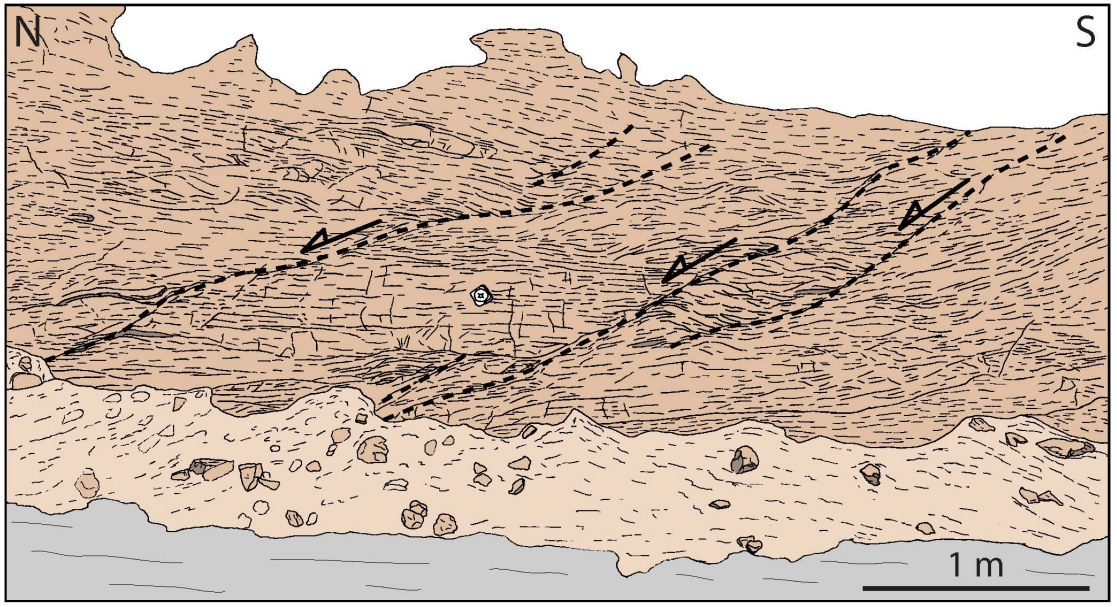
N
S
1 m


b

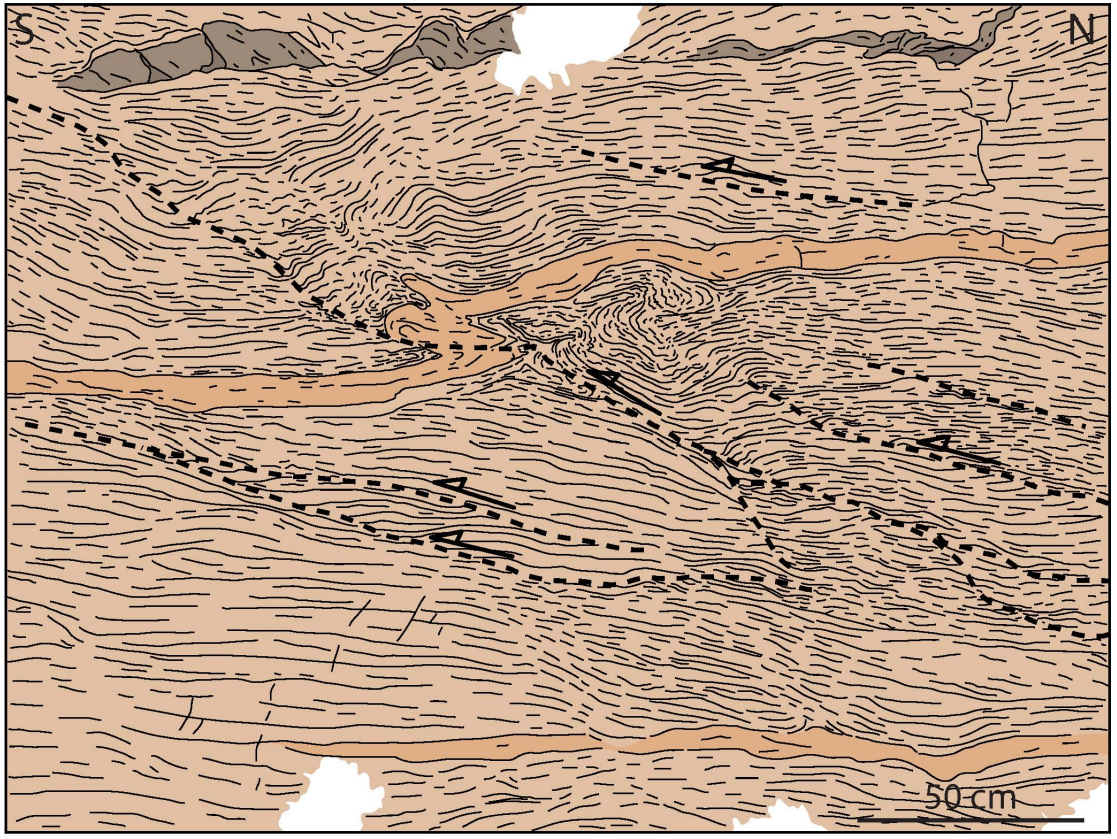
S
N
50 cm


c
b
a

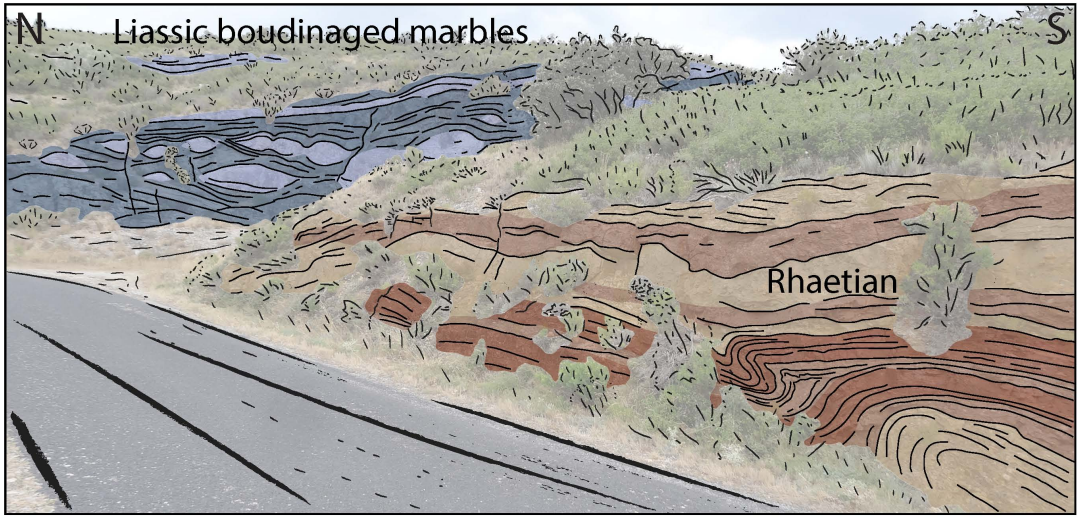
N
Liassic boudinaged marbles
S
Rhaetian


b


c

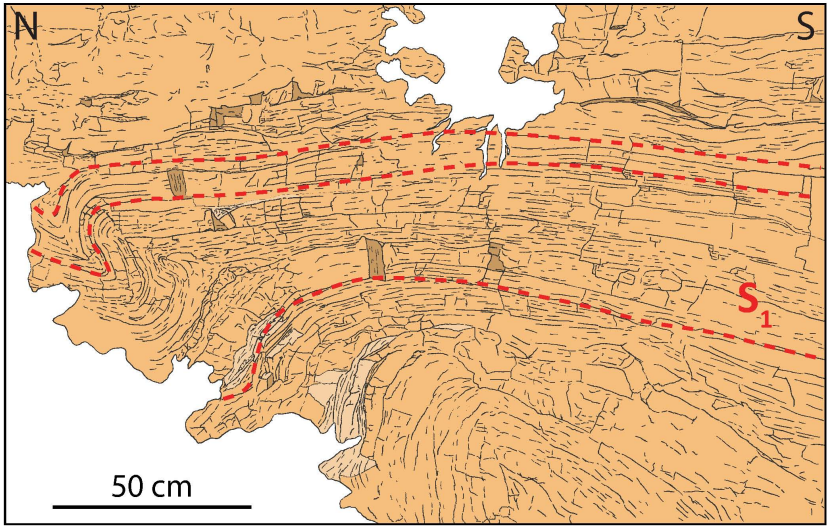
N
S
S1
50 cm

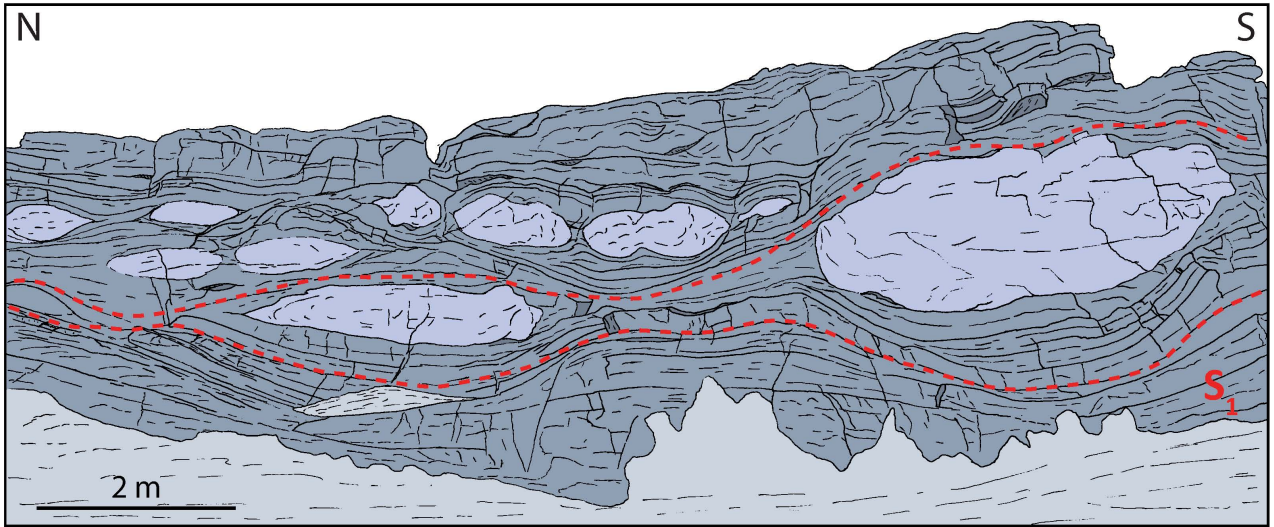
N
S
S1
2 m